






## Heat treatment of AM alloys

Author: Tuomas Riipinen

Confidentiality: Public

<b>Report's title</b> Heat treatment of AM alloys	
<b>Customer, contact person, address</b> Business Finland Porkkalankatu 1 00180 Helsinki	<b>Order reference</b> Business Finland Dnro 628/31/2018
<b>Project name</b> New business from digital spare parts	<b>Project number/Short name</b> 119165 - DIVALIITO
<b>Author(s)</b> Tuomas Riipinen	<b>Pages</b> 33 p.
<b>Keywords</b> Additive manufacturing, L-PBF, heat treatment, post processing, mechanical properties, microstructure	<b>Report identification code</b> VTT-R-00899-20
<b>Summary</b> <p>New commercial metal alloys are being gradually introduced to laser powder bed fusion (L-PBF) technology but the basic material portfolio has remained relatively constant over the years, comprising of steels (austenitic, tool steel, precipitation hardening), aluminum alloys (casting grades), titanium alloys, nickel superalloys, cobalt-chromium and few others. The active research on the process-material property interaction has increased the knowledge on the effect of processing conditions on the final material properties. There is however, no consensus on optimal heat treatment practices for AM parts, although heat treatment specifications for AM fabricated parts have been prepared in the form of ASTM standards for a several alloys. For heat treatment guidance of AM parts the SAE Aerospace Material Specifications (AMS) or existing ASTM heat treatment standards are typically referenced or adopted to AM alloys. However, the AMS specifications are not designed for L-PBF, which produces unique microstructures that often respond to heat treatment processes differently compared to wrought / cast alloys. Hence, these processes do not always lead to desirable material performance.</p> <p>This report provides a short review of the heat treatment practices employed for traditionally manufactured (cast / wrought) alloys as well as the practices recommended for AM alloys manufactured with L-PBF. The alloys discussed are 316L, Maraging, 17-4PH, H13, AlSi10Mg, Ti6Al4V, Inconel 625 and Inconel 718. The purpose is to provide information regarding each alloy and to provide a brief review of the heat treatment practices reported in literature and their effect on the microstructure and mechanical properties.</p>	
<b>Confidentiality</b>	Public
Espoo, 22.10.2020	
<b>Written by</b>  Tuomas Riipinen Research Scientist	<b>Reviewed by</b>  Sini Metsä-Kortelainen Senior Scientist
<b>Accepted by</b>  Pasi Puukko Research Team Leader	
<b>VTT's contact address</b> VTT Ltd, POB 1000, FI-02044 VTT, Finland, Tel. +358 20 722 111 (exchange)	
<b>Distribution (customer and VTT)</b> DIVALIITO steering group, pdf VTT archives, original and pdf	
<i>The use of the name of VTT Technical Research Centre of Finland Ltd in advertising or publishing of a part of this report is only permissible with written authorisation from VTT Technical Research Centre of Finland Ltd.</i>	

## Contents

1	Preface .....	3
2	General information .....	3
3	Steels.....	4
3.1	316L .....	4
3.2	Maraging (18Ni(300) / EN 1.2709) .....	7
3.3	17-4 PH .....	10
3.4	H13.....	12
4	Aluminum alloys.....	14
4.1	AlSi10Mg .....	14
5	Titanium alloys.....	17
5.1	Ti6Al4V.....	17
6	Nickel-based superalloys .....	20
6.1	Inconel 625 .....	20
6.2	Inconel 718 .....	23
7	Summary .....	26
8	Conclusions .....	28
	References.....	29

## 1 Preface

---

This report is a DIVALIITO project document for Performance and quality assurance of digital spare parts work package focusing on AM materials and post-processing steps needed, the properties of additively manufactured spare parts and the development of quality assurance procedures. In this report, the traditional heat treatment procedures and specifications for typical AM alloys are documented and the literature for heat treatment of AM alloys is briefly reviewed.

Espoo, July 2020

Tuomas Riipinen

## 2 General information

---

In order to better understand materials and material selection in the context of Additive Manufacturing (AM) and especially Laser Powder Bed Fusion (L-PBF), several essential process, material and quality related topics are explained briefly below. In L-PBF process the quality of the printed part is affected by the process parameters, powder properties, building process and the post processing steps. The process parameters include laser parameters, energy input and scanning strategy. The building process related properties include the consistency of the recoated powder layer, build chamber atmosphere, gas flow properties and platform heating. Powder properties comprise of chemical composition, particle size distribution, morphology, flowability, optical and thermal properties. The post-processing steps typically related to printed parts are heat treatment, part removal, machining and surface treatments.

In general, it is advisable to use feedstock powders that are tailored for AM and have undergone a quality control procedure to ensure the critical powder properties are within acceptable limits. Every L-PBF machine is unique and will produce a slightly different result compared even to other machines of similar model. Each machine manufacturer typically has a set of recommended process parameters for each material they support. The process parameters are designed to be robust enough to ensure good quality (low porosity and good geometric accuracy) despite the inevitable variability caused by the feedstock and building process. The layer-by-layer powder melting process creates microstructures unique to the L-PBF process that are hard to predict and the formed microstructure ultimately determines the mechanical properties of the material. The high temperature gradients during the manufacturing process create high internal stresses in the printed parts, the severity of which depends on parts size, material and process parameters. Due to this reason, L-PBF parts are typically stress relieved while still attached to the platform to avoid plastic deformation and cracking when the parts are removed. The microstructure of L-PBF parts is anisotropic, which should be considered when designing the part nesting and orientation. No matter how well all the different parameters are fine tuned there will always be some amount of defects in the printed parts. For non-critical parts that do not need to withstand high static or cyclic loads, higher defect density can be tolerated. However if the part is used in an application where fatigue properties are critical, very small amount of defects with specific size limitations can be accepted in the finished product. Surface roughness also influences the mechanical properties, which should be considered during the design phase.

Physical properties such as thermal, electrical and optical properties are similar between traditionally and additively manufactured as long the chemical compositions do not differ significantly. Direct comparison between AM and other manufacturing methods is not

straightforward in case of post processing. The purpose of heat treatments is to produce a microstructure in a manufactured part that provides certain material properties required for a given application. Therefore, the heat treatment parameters such as temperature, hold time and cooling rate are modified to tailor the mechanical properties of an alloy to suit specific needs.

This report is structured in a way that provides a general overview of the L-PBF alloys, the typical heat treatment practices used in industry for wrought / cast parts and the heat treatment specifications for L-PBF parts found in published AM standards. The effect of different heat treatment procedures on the microstructure and mechanical properties of each alloy based on published research articles are briefly reviewed. In addition, the mechanical properties of L-PBF manufactured alloys are reported based on information found in machine manufacturer's material data sheets.

### 3 Steels

---

#### 3.1 316L

316L is an austenitic molybdenum alloyed stainless steel grade that has a lower carbon content (max. 0.030 %) compared to 316 to prevent grain boundary carbide precipitation (sensitization). 316L is the alloy designation given by SAE International and the comparable material designations based on European and American standards are EN 1.4404, EN 1.4432 and EN 1.4435 and UNS S31603 respectively. The face-centered cubic (FCC) austenitic structure is obtained by addition of austenitizing elements such as nickel, manganese and nitrogen. The austenitic structure provides stability at low and at relatively high temperatures and is non-magnetic. Austenitic stainless steel grades form a passive film in the presence of oxygen at low temperatures that protects it in corrosive environments. The stability of this passive layer depends on the environment, and it is important to choose the material correctly.

The nominal material composition for the 316L is shown in Table 1 (UNS S31603), where single values indicate maximum values. Chromium is an essential element in forming a passive film that protects steel in corrosive environments. Chromium content between 17 and 20 % improves the stability of the passive film and although increased chromium content would increase the corrosion resistance, it may adversely affect the mechanical properties of the alloy. Molybdenum combined with chromium is effective in stabilizing the passive film in the presence of chlorides. [1] It also helps prevent the initiation of pitting and crevice corrosion. Nickel stabilizes the austenitic structure and greatly enhances the mechanical properties. Nickel additions of above 10 % improves the resistance to stress-corrosion cracking. Nickel also improves the corrosion resistance in mineral acids. Manganese has similar attributes as nickel in moderate quantities. Manganese forms sulfides that are beneficial for improving pitting corrosion resistance. [1]

316L is resistant to intergranular corrosion at a wide temperature range but prolonged exposures to high temperatures (650 to 870°C) is not recommended due to formation of  $\sigma$ -phase [2]. Tensile and yield strength of 316L can be improved by adding Nitrogen as alloying element and this grade is designated as 316LN.

*Table 1. Nominal chemical composition for the low carbon grade 316L austenitic stainless steel. [1]*

Element	C	Mn	Si	Cr	Ni	P	S	Mo
wt%	0.03	2.00	1.00	16-18	10-14	0.045	0.03	2-3

Austenitic stainless steels cannot be hardened by heat treatment and are typically delivered in annealed or cold-worked state, but also stress relieving is sometimes used. The material strain hardens upon cold work and increasing the amount of cold work (% reduction) results in higher yield- and tensile strengths while the ductility decreases. After severe plastic deformation the material should be annealed to restore ductility. Other function of annealing is to dissolve the chromium carbides that promote intergranular corrosion. Normalization is not recommended. [3]

Annealing is typically done at temperatures ranging from 1040°C to 1105°C, where suitable hold time depends on the thickness of the material. [3] Parts can be air cooled from the annealing temperatures, as the material is not susceptible to carbide formation during air cool [2]. Water quenching is however recommended for large section sizes [3]. In aerospace practice, parts are annealed at 1095°C and water quenched except for thin parts (<2.5 mm) that can be air cooled to prevent distortions. [3]

The main purpose of stress relieving for austenitic stainless steels is to prevent stress corrosion or intergranular corrosion failures. A temperature of 900°C is required for sufficient stress relief and the material can also be stress relieved at annealing temperatures followed by slow cool. [2] Parts can be water quenched from 900°C as is done in aerospace practice [3]. The effect of the stress relieve (% of stresses removed) depends on temperature and hold time, where hold times exceeding 2 h do not provide notable improvement in stress removal. At temperatures below 900°C only partial stress removal can be obtained, but stress relief temperatures as low as 370°C are still used to remove peak stresses. [2]

### *Additive manufacturing*

316L is a widely available material for L-PBF technology as it is easy to process and provides material properties (ductility, corrosion resistance) that make it suitable for many applications and use environments. Heat treatment guidance for 316L parts produced with powder-bed fusion is provided in the ASTM F3184-16 standard [4]. The standard specifies delivery conditions based on the thermal post-processing. The parts are either delivered in stress-relieved, solution annealed or Hot Isostatically Pressed (HIP) condition, but there is also option where all thermal post-processing is optional. Stress relief and solution annealing guidance is found in the SAE AMS 2759 and solution annealing in ASTM A484/484M standard. Parameters for HIP processing are provided in the F3184-16 standard and should at minimum conform to ASTM A1080 standard. For stress relief the temperature of 900°C provides maximum stress relief while the lower stress relief temperature below 400°C removes the peak stresses only. An intermediate temperature can be applied to achieve a compromise between stress removal while largely preserving the as-built microstructure. The current heat-treatment guidance for L-PBF parts largely follows the aerospace practices. The choice of thermal post processing method should be selected based on the end use application, which dictates the required properties, e.g. mechanical properties and corrosion resistance.

The as-built microstructure of L-PBF processed 316L is characterized by fine cellular solidification sub-structure and elongated grains that can extend through multiple layers due the thermal history induced by the manufacturing process [5]. Printed parts typically have high density ( $\geq 99.9\%$ ) in as-built condition, but can decrease when suboptimal process parameters are used. The L-PBF process parameters (laser power, scanning speed, hatching, scanning strategy, layer thickness) affect the forming microstructure and homogeneity of material after solidification [6], [7] and thus the mechanical properties of the material. Therefore using different machines with different process parameters results in multiple sources of variability that affect the material properties of L-PBF manufactured 316L.

The strength of the alloy is highest in the as-built condition due to the very fine cellular sub-structure with high dislocation density. The structure is highly anisotropic which differs greatly from wrought microstructure with homogenous grain structure and equiaxed grains. While the anisotropy and high strength might be useful in some applications, the homogenous microstructure and isotropic properties are still usually preferred. Heat treatment is therefore necessary to obtain a more isotropic structure while retaining good mechanical properties. HIP processing is often performed on AM parts to increase the material density and consequently the mechanical performance.

The results of a study on the effect of different heat treatments on the material properties of L-PBF manufactured 316L were published in a GE research report [8] focusing on nuclear applications. The same data was used in the publication by Lou, X. et al [9]. They employed the following heat treatments for as-built samples: Stress relief (650°C / 2 h in argon), HIP + solution anneal (HIP: 1150°C / 4 h, 1000 bar (argon) + SA: 1066°C / 1 h, water quench), partial recrystallization (955°C / 4 h, argon) and Solution anneal (1150°C / 2 h, argon). The purpose of solution annealing was to remove carbides that might precipitate during slow cooling after HIP processing.

The as-built structure with directionally solidified columnar (elongated) grains did not change after stress relieving and the stresses were only partially removed according to Electron Backscatter Diffraction (EBSD) measurements. The as-built and stress relieved microstructures had high dislocation density and dislocation entanglement (dislocation cell structure), small angle grain boundaries and nanoscale inclusions along columnar boundaries and in the material matrix (Mn and Si rich oxides) as identified by Transmission Electron Microscope (TEM) analysis. The oxides were larger (300 nm) after high temperature annealing and the HIP + SA processing. HIP + SA resulted in almost fully recrystallized structure consisting of equiaxed grains with annealing twins having average grain size of 70-100 µm. However, parts produced using different L-PBF system and same powder had a significantly different outcome after HIP + SA as a large fraction of unrecrystallized grains were observed in samples built using a different machine. [8] Similar observation was made by Puichaud, A. et al. [10] as L-PBF 316L samples after HIP (1100°C / 3 h, 1800 bar, argon, cooling 800°C/h) had a grain structure with approximately half of the grains remaining columnar and the rest recrystallized. HIP is shown to be effective in reducing porosity in AM samples [11].

Based on tensile test results reported in the GE report [8], the yield and tensile strengths were highest in the stress relieved condition and decreased after HIP + SA, whereas the ductility was improved. Considering all processing conditions, the AM material had a higher strength compared to wrought material and a reasonable elongation at break (minimum 40 % for stress-relieved parts in horizontal orientation) at room temperature [8].

After solution annealing at 1066°C for 1 h the yield, and tensile strengths were similar to HIP + SA condition but the ductility was slightly lower (higher porosity). The Charpy-V impact toughness tests showed that the impact energies are similar in stress relieved, HIP + SA and SA conditions (130-150 J). For wrought alloys the impact energies are typically 200 J or even higher. Scanning Electron Microscope (SEM) analysis revealed fracture surface typical for ductile fracture and oxide inclusions were observed in most of the dimples suggesting that the inclusions acted as initiation sites for microvoid formation reducing impact toughness. Oxygen contents of 326 ppm and 383 ppm were measured in the feedstock powder and printed parts, respectively, which is higher than what is typically measured in conventionally manufactured wrought and powder metallurgy (PM) 316L (100-200 ppm). [8] Oxygen content has been shown to decrease the impact toughness of PM-HIP 316L alloys [12].

The mechanical properties of conventionally manufactured and L-PBF fabricated 316L are compared in Table 2. The AM mechanical properties (SLM Solutions, EOS) are obtained from material data sheets.

Table 2. Mechanical properties of 316L.

	S31603, Forging, annealed <sup>1</sup>	316L, cold drawn bar	SLM Solutions, vertical, 30 µm (as-built) <sup>3</sup>	SLM Solutions, vertical, 30 µm (annealed) <sup>4</sup>	EOS, vertical, 40 µm (as- built) <sup>5</sup>
Young's modulus [GPa]	-	193	188 ± 17	188 ± 31	-
Yield strength [MPa]	170	380	491 ± 6	345 ± 4	500
Tensile strength [MPa]	450	585	582 ± 15	539 ± 15	590
Elongation [%]	40	45	49 ± 5	58 ± 5	46.7
Reduction in area [%]	-	-	72 ± 1	67 ± 4	-
Hardness	-	199 HV	204 ± 3 HV10	169 ± 3 HV10	-
Impact toughness [J]	-	103	-	-	-

<sup>1</sup> Forging, Annealed. ASTM A 473 specification. [1]

<sup>2</sup> AISI Type 316L Stainless Steel, annealed and cold drawn bar. [13]

<sup>3</sup> Vertical orientation. Layer thickness 30 µm. Tensile tests: ISO 6892-1:2017 B. Hardness measurements: DIN EN ISO 6507-1:2018. [14]

<sup>4</sup> Vertical orientation. Layer thickness 30 µm. Heat treatment: anneal at 1095 °C for 2 h, water quench. Tensile tests: ISO 6892-1:2017 B. Hardness measurements: DIN EN ISO 6507-1:2018. [14]

<sup>5</sup> EOS M290 system. Vertical orientation. Layer thickness 40 µm. [15]

### 3.2 Maraging (18Ni(300) / EN 1.2709)

Maraging steels, i.e. martensite aged hardening steels, are strengthened by precipitation of intermetallic compounds that do not contain carbon, at temperatures of about 480°C. Maraging steels have high yield strength and the martensitic structure formed after annealing is relatively soft (30-35 HRC) and dimensionally very stable during age hardening. The fracture toughness is considerably better than with conventional high-strength steels. Maraging steel have excellent weldability and are well suited for machining in the age hardened and solution annealed conditions. [1] Maraging steels (premium grades) are used extensively in aircraft and aerospace applications where excellent mechanical properties and weldability are key criteria. The usefulness of maraging steels in tooling applications comes from their excellent mechanical properties combined with lack of distortion during age hardening. Other applications include springs, bearings, transmission shafts, bolts, hydraulic hoses, punches, dies, couplings and fan shafts. [1]

Maraging steels have very high nickel, cobalt and molybdenum contents and very little carbon, which is considered as an impurity as it can form Titanium carbide that degrades mechanical properties. These materials have an iron-nickel lath martensite structure containing high dislocation density and are typically fully martensitic at room temperature. Some austenite is present in the heat-affected zone (HAZ) of welds that is sometimes used to improve the performance of the material in service, but austenite in the matrix degrades strength of the alloy. The main contribution of Cobalt is to lower the solubility of molybdenum in the martensitic



matrix increasing the amount of  $\text{Ni}_3\text{Mo}$  precipitate formed during age hardening. Molybdenum is the major precipitate former/hardener in maraging steels, which upon aging forms the  $\text{Ni}_3\text{Mo}$  phase. Addition of titanium promotes age hardening as it forms  $\text{Ni}_3\text{Ti}$  precipitates. [1]

The 18Ni(300) is among the most widely used maraging steel grades and the nominal chemical composition is shown in Table 3. In addition, other maraging varieties have been developed for specific purposes such as cast grades, stainless grades and cobalt free alloy for nuclear industry. Maraging steels are typically manufactured by air melting followed by vacuum arc melting or vacuum induction melting. Special low impurity grades used in e.g. aerospace applications require multiple melting steps. [1]

*Table 3. Nominal chemical composition of Maraging steel 18Ni(300). [1]*

Element	Ni	Mo	Co	Ti	Al
wt%	18	5	9	0.65	0.1

Prior to age hardening the maraging steels are solution annealed by heating and holding material austenite region for the amount of time it takes to dissolve the alloying elements into solid solution followed by cooling to room temperature. A typical solution anneal for 18Ni300 grade is to heat to 850°C for 1 h followed by air cool. The solution treatment temperature however has only a small effect on the strength of the alloy after age-hardening process. Maraging steels should be cooled to room temperature prior to age hardening, but the cooling rate does not have much effect on the microstructure and mechanical properties. For age hardening the alloy is heated to 455 to 510°C for 3-12 h followed by air cool. Hardening is very rapid and long hold times at aging temperature result in coarsening of the precipitates, i.e. overaging, which degrades the mechanical properties. [2]

#### *Additive manufacturing*

Maraging alloy 1.2709 is supported by most of the L-PBF machine providers and is mainly offered as a suitable material solution for tooling applications due to its high hardness and strength, decent ductility and the possibility to add cooling channels via the AM route. The strength of the material comes from the intermetallic precipitations formed during the age hardening heat treatment as explained above. Heat treatment guidance is not available in AM standards but some of the system manufacturers / powder suppliers have recommended certain heat treatment practices for their alloys. According to machine manufacturer's material data sheets the typical reported ageing process is to heat parts to 490-500°C, hold for 6 h and air cool. In some instances a furnace cool to 300°C followed by air cool to room temperature is mentioned, but also solution anneal at 940°C + ageing at 490°C has been reported (EOS) [16]. The mechanical properties for conventional and L-PBF fabricated maraging alloys are shown in Table 4.

Oter, Z.C. et al. [17] studied the microstructure of as-built maraging steel (EOS M290 system, EOS M1 powder) reporting a cellular grain structure with both equiaxed and columnar grains (epitaxial growth). Similar as-built microstructure was observed in L-PFB manufactured maraging steel by Mutua, J. et al. [18] who observed that the phase structure consisted of martensite as well as retained austenite. After solution anneal at 820°C the austenite transformed completely to martensite. After ageing at 460-600°C for 0.5-5 h no austenite was observed. The authors stated that after longer ageing treatment the decomposition of martensite into austenite could occur. Samples solution treated and aged at 460°C for 5 h had an average grain size of  $1.27 \pm 1.3 \mu\text{m}$  compared to  $0.982 \pm 0.961 \mu\text{m}$  of the as-built material. The hardness values after solution treatment and ageing at 480°C for 5 h / 460°C for 5 h were 593 HV and 610 HV, respectively, which is comparable to conventional age-hardened

maraging. Solution treatment and ageing increased the strength significantly compared to as-built material. The tensile strength after solution treatment and ageing at 460°C / 5h was 2033 MPa and elongation at break was 5.6 %. [18]

The influence of aging parameters and part orientation on mechanical properties of AM 18Ni300 maraging steel were reported by Mooney, et al. [19], to quantify the plastic anisotropy behavior of the alloy. They printed rectangular tensile test specimens in horizontal, 45° and vertical orientations (EOS M280 machine, EOS MS1 powder) and machined the samples prior to testing. They applied aging temperatures from 460° up to 600°C with different hold times. The authors reported that a notable increase of austenite formation was observed at cell boundaries due to austenite reversion process at aging temperatures of  $\geq 490^\circ\text{C}$ . Notable plastic anisotropy was present in the samples where the powder supplier's recommended heat treatment practice was followed. The mechanical properties can be tailored for specific needs by underaging or overaging the structure to increase strength or toughness. As an optimal aging practice providing high strength and isotropy, the authors recommended aging at 490°C for 8h and for isotropy, higher ductility and lower strength requirement aging at 525° for 8h was suggested.

Table 4. Mechanical properties of 18Ni 300 maraging steel.

	18Ni300 (solution treated + aged) <sup>1</sup>	SLM Solutions, vertical, 30 $\mu\text{m}$ (As-built) <sup>2</sup>	SLM Solutions, vertical, 30 $\mu\text{m}$ (Heat treated) <sup>3</sup>	EOS, vertical, 40 $\mu\text{m}$ (Heat treated) <sup>4</sup>	EOS, horizontal, 40 $\mu\text{m}$ (Heat treated) <sup>4</sup>
Young's modulus [GPa]	-	181 $\pm$ 2	204 $\pm$ 4	-	-
Yield strength [MPa]	2000	1076 $\pm$ 15	1937 $\pm$ 17	2180	2170
Tensile strength [MPa]	2050	1213 $\pm$ 20	2111 $\pm$ 20	2260	2250
Elongation [%]	7	10 $\pm$ 2	4 $\pm$ 2	3.3	4.2
Reduction in area [%]	49	49 $\pm$ 3	19 $\pm$ 5	-	-
Hardness	-	354 $\pm$ 8 HV10	608 $\pm$ 5 HV10	57 HRC	
Impact toughness [J]	-	-	-	10	
Fracture toughness [MPa*m <sup>1/2</sup> ]	80	-	-	-	-
Fatigue strength [MPa]	-	-	-	732	

<sup>1</sup> Solution heat treated at 815°C for 1 h + aged at 480 °C for 3 h. [2]

<sup>2</sup> Vertical orientation. Layer thickness 30  $\mu\text{m}$ . Tensile tests: ISO 6892-1:2017 B, hardness measurements: DIN EN ISO 6507-1:2018. [20]

<sup>3</sup> Vertical orientation. Layer thickness 30  $\mu\text{m}$ . Heat treatment: Heat treatment: aging 500 °C, 6 h; air-cooling. Tensile tests: ISO 6892-1:2017 B, hardness measurements: DIN EN ISO 6507-1:2018. [20]

<sup>4</sup> EOS ToolSteel 1.2709, M 290 system. Vertical and horizontal orientations. Heat treatment: solution anneal at 940 °C ( $\pm 10$  °C) for 2 h (cooling rate 10-60 °C/min) + ageing at 510 °C ( $\pm 10$  °C) for 3-6 h, air cool. Tensile tests: ISO6892-1. Hardness measurements: ISO6508. Impact toughness tested according to ISO 148-1, V-notch at room temperature. Fatigue tests: ASTM E466 (Fatigue strength at 1 x 10<sup>7</sup> cycles in heat treated state). [21]

### 3.3 17-4 PH

Precipitation hardening (PH) stainless steels are divided into martensitic (17-4 PH, 15-5 PH), semi-austenitic (PH 15-7, 17-7 PH, AM 350, AM 355) and austenitic grades (E630, ER630) [1]. In the martensitic grades such as the 17-4PH, austenite transforms to martensite upon cooling to room temperature. The structure is strengthened by aging process where second phase precipitates are formed from the supersaturated martensitic matrix giving the material high strength and ductility. Chromium gives corrosion resistance and also decreases the rates of certain transformations [22]. Nickel is added to stabilize austenite and to improve corrosion resistance. Copper, molybdenum, titanium, niobium and aluminum form precipitates from solid solution during ageing. Controlling the composition is essential to avoid formation of  $\delta$ -ferrite during solution annealing and retained austenite after cooling. [1] 17-4 PH is cast in plastic-bonded shell molds [2] or forged to form from ingot. The material properties of finished product can be altered by changing the heat treatment parameters, but typically the alloy is solution treated at temperatures ranging from 1025°C to 1050°C and oil quenched to room temperature, followed by aging at 480°C for 1 h and air cooled (H900) resulting in hardness of 42-44 HRC [3]. The material can be homogenized before solution annealing by holding at 1149°C for at least 90 min [2].

Table 5. Nominal chemical composition of 17-4 PH alloy (UNS S17400). [2]

Element	C	Mn	P	S	Si	Cr	Ni	Cu	Nb
wt%	max. 0.07	max. 1.00	max. 0.04	max. 0.03	max. 1.00	15-17.5	3.0-5.0	3.0-5.0	0.15- 0.45

#### *Additive manufacturing*

The combination of strength and ductility together with corrosion resistance makes 17-4 PH steel an attractive choice for demanding applications and is an integral part of the material portfolio for L-PBF. The rapid solidification during L-PBF creates an as-built structure with very fine dendrites and columnar grains while the phase structure is mostly martensitic with some retained austenite [23].

Studies have shown that the L-PBF processed 17-4 PH is not fully martensitic and consists of varying fractions of retained austenite, where parts processed under nitrogen atmosphere have more retained austenite compared to using argon as protective gas. [7, 8] In a more recent publication, Meredith, S.D. et al. [25] studied the effect of feedstock composition on the properties of L-PBF manufactured 17-4 PH. Two powder lots atomized in N<sub>2</sub> and argon gas were used to manufacture test samples in build chambers with N<sub>2</sub> and argon atmospheres. The powders atomized in argon had low levels of retained austenite, which remained low in the as-built samples. The N<sub>2</sub> atomized powders had considerably higher amounts of retained austenite, which decreased in the printing process. The argon atomized powder that contained low amounts of nitrogen (0.01 %) and retained austenite (> 1 %) responded to heat treatment similarly to wrought material. Higher amounts of retained austenite in the feedstock powder and hence is printed parts was attributed to higher nitrogen concentration of the feedstock powders whereas the effect of N<sub>2</sub> shielding gas in the printing process was not considered significant.

The effect of heat treatments on the microstructure of 17-4 PH was studied by Sun, Y. et al. [26]. The as-built structure consisted of columnar ferrite grains with fine grains of austenite and martensite around the melt pool boundaries. The material contained approximately 4 % retained austenite based on EBSD analysis. The printed microstructure differed greatly from

wrought microstructure comprising of lath martensite. After solution annealing and ageing heat treatment (H900) the printed parts obtained relatively homogenous fine martensitic grain structure where the fraction of the austenite phase was 2.5%. The microstructure of heat-treated AM part resembled that of wrought and heat-treated alloy except the grain structure being more refined. The AM part also contained more oxide inclusions and larger precipitates that were also observed at the grain boundaries.

Research by Elwany, A. et al. [27] on the effect of process conditions on the mechanical properties of 17-4PH showed that the L-PBF manufactured (3D systems ProX 100 machine, powder by 3D Systems) and heat treated (H900 = solution anneal at 1038°C / 0.5 h + AC, aging at 482°C / 0.5 h + AC) samples had lower ductility, tensile and yield strengths compared to wrought alloy (H900). Horizontally oriented test samples had higher strength ( $R_{m(\text{horizontal})} \approx 1250$  MPa,  $R_{m(\text{vertical})} \approx 950$  MPa,  $R_{m(\text{wrought})} \approx 1300$  MPa) and ductility ( $A_{\text{horizontal}} \approx 8\%$ ,  $A_{\text{vertical}} \approx 4\%$ ,  $A_{\text{wrought}} = 10\%$ ) compared to vertically oriented samples after heat treatment which the authors attributed to weaker interfacial layers (microstructural defects) in the vertically oriented samples. The amount of retained austenite for both samples was measured as 16.3%. The authors also observed that individually built samples had higher amount of retained austenite compared to samples built as part of a batch. Shorter waiting times between scans of the individually manufactured parts produced a more coarse austenitic structure due to higher part temperature during the manufacturing process. Heat treating improves the strength of the alloy but reduces ductility, and process parameters that reduce the defect density are important in improving the mechanical properties. [27]

Mechanical properties of cast and printed 17-4 PH alloy are shown in Table 6. The mechanical properties of AM alloys are obtained from the material data sheets.

Table 6. Mechanical properties of 17-4 PH alloy.

	17-4 PH, wrought (H900) <sup>1</sup>	17-4 PH, cast (H900) <sup>2</sup>	SLM Solutions, 30 µm, vertical (As-built) <sup>3</sup>	SLM Solutions, 30µm, vertical (H900) <sup>4</sup>	SLM Solutions, 50µm, vertical (H900) <sup>5</sup>	EOS, vertical, 40µm (Vacuum H900) <sup>6</sup>	EOS, horizontal 40µm (Vacuum 460°C) <sup>7</sup>
Young's modulus [GPa]	-	-	154 ± 19	182 ± 4	151 ± 5	-	-
Yield strength [MPa]	1170	1055	506 ± 25	1091 ± 27	866 ± 41	1251 ± 14	1262 ± 13
Tensile strength [MPa]	1310	1380	931 ± 45	1308 ± 88	1189 ± 16	1343 ± 8	1358 ± 7
Elongation [%]	10	15	28 ± 2	14 ± 6	22 ± 1	14 ± 1	14 ± 1
Reduction of area [%]	40		56 ± 8	26 ± 17	53 ± 5	-	-
Hardness	40 HRC	44 HRC	226 ± 2 HV10	352 ± 22 HV10	367 ± 24 HV10	42 ± 1 HRC	43 ± 1 HRC

<sup>1</sup> 17-4 PH (UNS S17400) Bar, Forgings. H900 heat treatment. [1]

<sup>2</sup> Alloy with 0.40 % Niobium. Heat treatment: homogenization 1150°C/1.5h air cool + solution anneal 1040°C/0.5h oil quench + aging 480°C/1h air cool. [2]

<sup>3</sup> Vertical orientation. Layer thickness 50 µm. Tensile test: ISO 6892-1:201. Hardness: DIN EN ISO 6507-1:2018. [28]

<sup>4</sup> Vertical orientation. Layer thickness 30 µm. Heat treatment: Solution annealing at 1040 °C for 30 min 2. Ageing at 480 °C for 60 min (H900). Tensile test: ISO 6892-1:201. Hardness: DIN EN ISO 6507-1:2018. [28]

<sup>5</sup> Vertical orientation. Layer thickness 50  $\mu\text{m}$ . Heat treatment: Solution annealing at 1040  $^{\circ}\text{C}$  for 30 min 2. Ageing at 480  $^{\circ}\text{C}$  for 60 min (H900). [28]

<sup>6</sup> EOS M290. Vertical orientation. Layer thickness 40  $\mu\text{m}$ . Heat treatment (vacuum, H900): Solution anneal: 1040 $^{\circ}\text{C}$  / 0,5 h, Air cool + Ageing: 480 $^{\circ}\text{C}$  / 1 h, Air cool. Tensile testing according to ISO 6892 & ASTM E8M. Rockwell Hardness, HRC, according to ISO 6508. [29]

<sup>7</sup> EOS M290. Horizontal orientation. Heat treatment (vacuum): Solution anneal: 1040 $^{\circ}\text{C}$  / 0,5 h, Air cool + Ageing: 460 $^{\circ}\text{C}$  / 1 h, Air cool. Tensile testing according to ISO 6892 & ASTM E8M. Rockwell Hardness, HRC, according to ISO 6508. [29]

### 3.4 H13

H13 is a hot-work tool steel having very high strength, toughness and decent wear resistance and the material retains its high strength and hardness at elevated temperatures. The alloy obtains its strength from vanadium carbides that precipitate in the martensitic matrix during tempering heat treatment (secondary hardening). Tensile strengths exceeding 2070 MPa are achievable by heat treatments. The alloy is used mainly in dies and other hot-work applications for its resistance to thermal fatigue and wear but it is also used in structural parts. At elevated temperatures the parts should be protected from corrosion by applying a protective coating. The material is delivered as bar, billet, rod and forgings. H13 parts can also be manufactured via powder metallurgy (PM) processing with the advantages of near net shape manufacturing and segregation free structure. [1]

H13 can be annealed for fully spheroidized structure by heating uniformly to 860-900 $^{\circ}\text{C}$  in a controlled atmosphere to avoid decarburization and cooling slowly to 480 $^{\circ}\text{C}$  (cooling rate not exceeding 30 $^{\circ}\text{C}/\text{h}$ ) [3] and then cooling more rapidly to room temperature. In order to obtain high strength the material is hardened and tempered. For hardening the alloy is preheated slowly (max. 110 $^{\circ}\text{C}$  / h) to 790-815 $^{\circ}\text{C}$  and the furnace temperature is then raised to 995-1025 $^{\circ}\text{C}$  for 20-40 min depending on the material thickness followed by air cool. For tempering the material is heated to 510 $^{\circ}\text{C}$  for 2 h for maximum hardness and air cooled. The tempering process is repeated for optimal mechanical properties. Higher tempering temperatures can be used (up to 650 $^{\circ}\text{C}$ ) for higher ductility and lower strength and hardness. For stress relieving it is recommended to heat to 650-675 $^{\circ}\text{C}$  and hold for 1 h followed by slow cool to room temperature. Stress relieving is typically done after rough machining and prior to finishing machining after which the material is hardened and tempered. [2]

Table 7. Nominal chemical composition of H13 alloy. [1]

Element	C	Mn	Si	Cr	Ni	Mo	V
wt%	0.32-0.45	0.20-0.50	0.80-1.20	4.75-5.50	0.30 max	1.10-1.75	0.80-1.20

#### *Additive manufacturing*

H13 is an attractive material for AM as it can be manufactured relatively well and is a good material for dies and other applications where high strength and good high temperature fatigue resistance are important. The microstructure of H13 in as-built condition was reported by Deirmina, F. et al. [30] to consist of alternating layers of quenched and tempered martensite, where certain layers underneath the solidifying layer may get tempered by the conducted heat. The solidification structure of H13 is reported to be cellular/dendritic [30, 31] with segregation of heavy elements at melt pool boundaries and micro-segregation of elements around cell boundaries [30]. According to Deirmina et al. [30] the printed material consists of martensite and retained austenite (19 vol.%) based on XRD analysis. Retained austenite was observed at the cellular boundaries where stabilization of austenite occurred due to segregation of solute elements. Samples quenched from austenite region (1020 $^{\circ}\text{C}$  / 15 min) had a homogenous structure consisting almost entirely of martensite. Quenched and double tempered (500 $^{\circ}\text{C}$  and

600°C), samples had a homogenous structure of tempered martensite and fine carbide precipitates, although some carbide network was observed around prior austenite grain boundaries. Retained austenite was observed in the material directly double tempered after printing at 500°C, but not after tempering at 600°C. In both cases, the cellular/dendritic structure was retained but less so after tempering at 600°C, which resulted in more homogenous structure. The hardness of printed and tempered material was higher compared to quenched and tempered (~460 HV1 vs. ~390 HV1). Fracture toughness was lower for samples with the notch plane normal to the build plane for both heat treatments. Fracture toughness for quenched and tempered samples with notch plane parallel and normal to the build plane were  $71.3 \pm 3.2 \text{ MPam}^{1/2}$  and  $80.3 \pm 1.3 \text{ MPam}^{1/2}$ . [30]

Reserccj by Narvan, M. et al. [31] point out the importance of using platform preheating when manufacturing tool steels using L-PBF. Printed parts showed large cracks when platform preheating was not applied and preheating the platform to 200°C resulted in crack free parts and increased the relative density of printed parts. Åsberg, M. et al. [32] reported on the effect of heat treatments on the mechanical properties of L-PBF manufactured H13. Stress relieved (650°C / 8 h), quenched (1020°C / 70-75 min) and double tempered (585 °C / 2.25–3 h) material had high strength (Yield strength = 1447 MPa, Tensile strength = 1640 MPa, Hardness = 511 HV20) and relatively low elongation at fracture (3.3 %). Performing HIP (1130°C / 6 h, 100 MPa) before quench and tempering resulted in higher strength (Yield strength = 1502 MPa, Tensile strength = 1743 MPa, Hardness = 562 HV20) and higher ductility (6.6 %). Higher strength and ductility after HIPping was attributed to significantly lower porosity compared to the other heat treatment conditions, which was confirmed by porosity analysis and fractography on the tested samples. The mechanical properties of conventionally and additively manufactured H13 are shown in Table 8. Some of the data from the machine manufacturer’s material data sheet is missing possibly due to the low ductility of the material. In general printed H13 has comparable or higher strength compared to wrought / PM alloy, but is also slightly less ductile. Some inhomogeneities such as porosity and segregation of alloying elements often remain even after austenitizing and tempering affecting the material properties of printed material. [32]

*Table 8. Mechanical properties on conventional and AM H13.*

	H13, Wrought <sup>1</sup>	H13, P/M <sup>2</sup>	SLM Solutions, 30µm, horizontal (As-built) <sup>2</sup>	SLM Solutions, 30µm, vertical (As-built) <sup>2</sup>	SLM Solutions, 30µm, horizontal (Heat-treated) <sup>3</sup>	SLM Solutions, 30µm, vertical (Heat-treated) <sup>3</sup>
Young's modulus [GPa]			203 ± 23	-	-	-
Yield strength [MPa]	1413	1407	987 ± 39	-	1528 ± 32	-
Tensile strength [MPa]	1696	1682	1244 ± 106	1360 ± 86	1719 ± 239	1720 ± 99
Elongation [%]	12	11	2 ± 2	1 ± 2	4 ± 2	9 ± 2
Reduction of area [%]	43	42	-	-	14 ± 5	16 ± 5
Impact toughness [J]	13.6	13.6	-	-	-	-
Hardness	46.0-47.7 HRC	47.5-48.1 HRC	-	-	-	-

<sup>1</sup> Longitudinal. Test temperature 21°C. Preheated at 816 °C, austenitized at 1010 °C / 1 h, air cooled. Tempered at 593°C for 2+ 2 h. [1]

<sup>2</sup> Vertical and horizontal orientations. Layer thickness 30 µm. Tensile tests according to DIN EN ISO 6892-1:2017 B.

<sup>3</sup> Vertical and horizontal orientations. Layer thickness 30 µm. Tensile test according to DIN EN ISO 6892-1:2017 B. Heat treatment: preheating to 750 °C for 2 h, followed by austenitizing at 1050 °C for 15 min. and quenching in warm oil (about 60 °C). Immediate double tempering at 300 °C for 2.5 h with interstage cooling down to room temperature.

## 4 Aluminum alloys

---

### 4.1 AlSi10Mg

AlSi10Mg is a casting aluminum alloy group comprising of different alloys, which according to SFS-EN 1706 standard, are designated by the number EN AC-43xxx based on chemical composition. The chemical composition for EN AC-43000 and EN AC-43100 alloys, also referred by the chemical symbols EN AC-Al Si10Mg(a) and EN AC-Al Si10Mg(b) consecutively, are shown in Table 9, where single values indicate maximum composition values and values in brackets are ingot compositions. American alloy with similar composition to the European alloy designations according to ASTM B179 standard is UNS A03602 [33]. Due to its low density and good mechanical and thermal properties the alloy is often used in aerospace and automotive components with thin and complex features.

Casting aluminum alloys contain considerably more Silicon (typically < 12 wt%) compared to wrought alloys as, in addition to increasing strength, makes casting possible by increasing fluidity, improving feeding characteristics and reducing cracking [34]. Magnesium is the main contributor to increasing the strength and hardness of Al-Si alloys through the formation of the Mg<sub>2</sub>Si hardening phase. Magnesium additions above to solubility limit of ~0.7 % does not provide further strengthening. Copper also increases the strength, hardness and improves hot tear resistance of Al-Si alloys but also reduces the corrosion resistance and castability. Iron improves hot tear resistance and strength by the formation of insoluble intermetallic phases. Aluminum alloys have good corrosion resistance due to the formation of oxide film on the surface, which reforms automatically when broken in most environments. [35]

Generally only precipitation hardenable aluminum alloys are heat treated by solution heat treatment, which is done by first dissolving the elements into solid solution followed by quenching to supersaturate the matrix and finally hardening by ageing to precipitate the hardening phases. [36] For AlSi10Mg the temper T6 is typically used, which is the designation for solution heat treatment and artificial ageing commonly at a temperature range of 150 to 200°C. Solution anneal temperatures and soak times depend on the alloy composition and for casting alloys longer soak times are used compared to wrought alloys due to the relatively large size of the microconstituents after casting [36]. Solution annealing temperature must be sufficient (above the solvus temperature) to achieve a nearly homogenous solid solution without exceeding the eutectic melting temperature. Soaking the parts at 530-540°C for 10 to 14 h should be sufficient for solution anneal as the solubility of Mg at 540°C is approximately 0.6 %. Quenching of aluminum castings is often done to hot water (60-80°C) in order to minimize quenching stresses. The choice of ageing parameters affect the size and distribution of precipitates and is therefore a compromise between different material properties such as tensile strength, yield strength and corrosion resistance. If the precipitates grow too large, i.e. the material is overaged, the mechanical properties begin to decrease. [2]

Stress relieving can be done after quenching to remove the quenching stresses as age hardening temperature is typically not sufficient to remove the stresses. Higher temperatures

results in more effective stress relief and in lower mechanical properties. Annealing at 315-345°C for 2-4 h relieves residual stresses of cast alloys effectively. [2]

*Table 9. Nominal chemical composition of EN AC-43000 alloys. [37]*

	Si	Fe	Cu	Mn	Mg	Ni	Zn	Pb	Sn	Ti	Others	Al
EN AC-43000 <sup>1</sup>	9.0-11.0	0.55 (0.40)	0.05 (0.03)	0.45	0.20-0.45 (0.25-0.45)	0.05	0.10	0.05	0.05	0.15	0.15	remainder
EN AC-43100 <sup>1</sup>	9.0-11.0	0.55 (0.45)	0.10 (0.08)	0.45	0.20-0.45 (0.25-0.45)	0.05	0.10	0.05	0.05	0.15	0.15	remainder
UNS A03602 <sup>2</sup>	9.0-10.0	0.70-1.10	0.10	0.10	0.45-0.60	0.10	0.10	-	0.10	-	0.20	remainder

<sup>1</sup> SFS-EN 1706. [37]

<sup>2</sup> ASTM B179(96). [33]

### *Additive manufacturing*

AlSi10Mg alloy is the most commonly available and used aluminum alloy in L-PBF manufacturing. The AM standards ASTM F3318-18 [38] and F3301-18 [39] provide thermal post treatment parameters for L-PBF manufactured AlSi10Mg alloy. According to the standards, parts shall be delivered either in as-built, stress relieved, solution annealed and aged (T6) or HIP + T6 condition.

The as-built microstructure of AM AlSi10Mg alloy differs from as cast microstructure considerably. Casting results in the formation of large dendrites ( $\alpha$  - Al) in an eutectic Al-Si matrix with Mg-rich intermetallic phases whereas the printing results in the formation of a metastable microstructure consisting of very fine grains inside the solidified melt pools and more coarse grains at the melt pool HAZ. After T6 heat treatment, the cast alloy has an even distribution of precipitates formed in the aluminum matrix. [40] In the case of L-PBF processed alloy, the formation of very fine grain structure is promoted by the high cooling rates of solidifying melt pools and the high thermal conductivity. Melting the top layer also heats the already solidified layers below providing aging effect, which promotes growth of Mg-rich precipitates [41]. Li, Z. et al. [42] reported that the cellular as-built structure of AlSi10Mg begins to break up after 4 min at stress relieving temperature (300°C) and that after 40 min the cellular structure was removed even further along with coarsening of Si precipitates. The fully cellular as-built structure exhibited significantly higher work hardening capacity compared to the more ductile heat-treated samples.

Pola, A. et al. [43] investigated the effect of different solution annealing and aging parameters on the microstructure and mechanical properties of L-PBF manufactured AlSi10Mg (EOS AlSi10Mg powder, EOS M290 system, layer thickness 30 $\mu$ m). The as-built structure with fine Al-rich cellular grains surrounded by Si particles coarsened after solution heat treatment. Increased solution heat treatment temperature and hold time reduced the amount of Si particles per unit area but also coarsened the particles. The average area of Si particles after 1 h at 480, 510 and 540°C was approximately 3  $\mu$ m<sup>2</sup>.

The as-built material is significantly harder than cast alloy and the hardness drops to comparable hardness values after solution heat treatment. According to research by Girelli, L. et al. [43] solution treatment at 480°C is not effective at dissolving elements into solid solution, thus resulting in lower hardness after quenching compared to higher temperatures, whereas



solution treatment at 510°C and 540°C resulted in similar strength after quench. The authors reported that soaking times between 1-3 h resulted in slightly higher hardness (~70 HBW) than with longer soaking times. After ageing at 160°C for 4 h the samples solution treated at 510°C and 540°C had higher hardness values compared to sample heat treated at 480°C, approximately 100 HBW regardless of solution treatment soaking time (1-9 h). For cast alloy, the hardness after the same ageing process varied from ~80 HBW (480°C) to around 100 HBW (540°C). According to the authors the material density decreased after solution treatment, where the effect was most notable after solution treatment at 540°C, where the porosity increased from 1 % to 4 % when soaking time increased from 1 to 9 h [43]. Similar observation of decreasing density was made by [44] concluding that the porosity increase resulted from growth of hydrogen porosities at temperatures exceeding 525°C. The solution treatments 480°C / 6 h, 510°C / 3 h and 540°C / 1 h were considered optimal by Girelli, L. et al. [43] in terms of hardness and material density. The following heat treatment process produced a good combination of hardness (>100 HBW) and density (2.641 g/cm<sup>3</sup>): Solution anneal at 510°C for 3 h, water quench and ageing at 160°C for 8 h. Also ageing at 180°C for 1 h produces a similar result. The authors performed tensile test on samples solution annealed at 540°C for 1 h and aged at 180°C for 2 h (Hardness = 111 ± 7 HBW) obtaining the following properties for horizontally (H) and vertically (V) oriented samples: Tensile strength (MPa) = 332 ± 1 (H) / 299 ± 24 (V), Yield strength (MPa) = 277 ± 1 (H) / 248 ± 14 (V), Elongation (%) = 5.8 ± 0.2 (H) / 5.1 ± 1.1 (V).

Garmendia, X. et al. [45] conducted tensile tests on L-PBF manufactured (Renishaw AM400 system, powder from LPW Technology Ltd., layer thickness = 30 µm) and subsequently machined AlSi10Mg samples. The samples were heat treated in accordance to the ASTM F3318-18 standard, i.e. solution treated at 530°C for 6 h followed by water quench and artificial ageing at 160°C for 6 h. The mechanical properties were the following: Tensile strength = 310 ± 4.4 MPa, Yield strength = 244 ± 3.1 MPa, Elongation at break = 9.2 ± 0.5 %. The authors demonstrated that coating the feedstock powder particles with 1% copper using a copper formate – methanol solution, resulted in notably better mechanical properties. Tensile specimens fabricated using the powder had 51 MPa higher ultimate tensile strength after the same heat treatment compared to the uncoated powder as a result of microstructural changes, such as smaller grain size.

Table 10. Mechanical properties of cast and AM AISi10Mg alloys.

	EN AC-43000, As-cast <sup>1</sup>	EN AC-43000, T6 <sup>1</sup>	SLM Solutions, 30µm, vertical (As-built) <sup>2</sup>	SLM Solutions, 30µm, vertical (Heat-treated) <sup>3</sup>	EOS, 30µm, vertical (as-built) <sup>4</sup>	EOS, 30µm, vertical (Stress relieved) <sup>5</sup>
Young's modulus [GPa]	-	-	75 ± 3	52 ± 4	-	-
Yield strength [MPa]	80 (min)	180 (min)	276 ± 5	150 ± 6	225	230 ± 20
Tensile strength [MPa]	150 (min)	220 (min)	482 ± 15	264 ± 10	350	470 ± 20
Elongation [%]	2 (min)	1 (min)	5 ± 2	11 ± 5	9	6 ± 2
Reduction of area [%]	-	-	-	-	-	-
Impact toughness [J]	-	-	-	-	-	-
Hardness	50 HBW (min)	50 HBW (min)	-	-	-	-

<sup>1</sup> Values are the minimum mechanical properties as stated in SFS-EN 1706 for sand cast test pieces. [37]

<sup>2</sup> Vertical orientation. Layer thickness 30µm. Tensile test: ISO 6892-1:2018. Hardness: DIN EN ISO 6507-1:2018. [46]

<sup>3</sup> Vertical orientation. Layer thickness 30µm. Tensile test: ISO 6892-1:2018. Hardness: DIN EN ISO 6507-1:2018. Heat treatment: anneal for 90 min at 270 °C. [46]

<sup>4</sup> Vertical orientation. Layer thickness 30µm. EOS M290. Tensile testing according to ISO 6892-1 B10, proportional test pieces. [47]

<sup>5</sup> Vertical orientation. Layer thickness 30µm. EOS M290. Heat treatment: anneal for 90 minutes at 270 °C. Tensile testing according to ISO 6892-1 B10, proportional test pieces. [47]

## 5 Titanium alloys

### 5.1 Ti6Al4V

Ti6Al4V is the most commonly used alpha-beta alloy in the world. The alloy has low density compared to steels, high strength, biocompatibility and good corrosion properties and is therefore extensively used in aerospace (gas turbine disks and blades, airframe structural components) and medical applications. Pure titanium has a hexagonal close-packed (HCP) crystal structure (alpha (α) phase) at room temperature, which at 883°C transform into body-centered cubic (BCC) structure (beta (β) phase). By adding alloying elements, the α-β transformation temperature broadens to a temperature range where both phases are in equilibrium. The final properties of α-β alloys are achieved after heat treatment where the alloy is cooled rapidly from the α-β phase region (solution treatment) and subsequently aged to produce mixture of α and transformed β phase. The microstructure and the final material properties can be altered by changing the solution anneal temperature (amount of β-phase) and cooling rate. The alloying elements are divided into alpha and beta stabilizers based on their effect on the alpha-to-beta transformation temperature. Aluminum is the primary α-stabilizer (raises the alpha-to-beta temperature), increasing the tensile strength, creep strength and elastic modulus. Aluminum content is typically limited to 6 wt% as a larger amount

promotes the formation of brittle  $Ti_3Al$  phase. Other alpha stabilizers are carbon, gallium, germanium, oxygen and nitrogen, where nitrogen and oxygen are considered impurities. Vanadium is a beta stabilizer along with iron, chromium, molybdenum and manganese. Nominal chemical compositions for Ti6Al4V and Ti6Al4V ELI (Extra low interstitial = lower levels of oxygen, nitrogen, carbon, iron) alloys are shown in Table 11. Formation of nonequilibrium phases such as the alpha-prime and metastable beta have a considerable strengthening effect on the alloy after heat treatment. Titanium's high affinity to oxygen makes it very reactive material but it also provides corrosion resistance due to formation of thin oxide film when exposed to air or other oxidizing environments. [35]

Suitable Ti6Al4V heat treatment is chosen based on the desired microstructure and material properties. Ti6Al4V is most often delivered in fully annealed condition (mill annealed). Annealing in the  $\alpha+\beta$  range creates a lamellar microstructure that has good fracture toughness and resistance to stress corrosion, crack growth and creep. [36] Solution treatment above  $\beta$ -transus and subsequent quench results in the formation of an acicular  $\alpha'$  martensitic structure or in mixed  $\alpha + \alpha'$  when quenched from 900-1000°C (below  $\beta$ -transus temperature). The  $\beta$ -transus temperature for Ti6Al4V is approximately 1000°C  $\pm$  20°C. Typical solution treatment temperature range and hold time for the Ti6Al4V for maximum tensile properties are 955-970°C and 1 h (water quench). [2] The solution treated alloy is further strengthened by aging at 480-595°C for 4-8 h, which decomposes the metastable  $\beta$  phase into  $\alpha$  [2]. Aging at higher temperatures produces an overaged microstructure which provides a modest increase in strength while maintaining decent toughness. Slow cooling from the  $\beta$ -phase to  $\alpha+\beta$  region results in a lamellar structure due to nucleation and growth of  $\alpha$  in the  $\beta$  grain boundaries. The microstructure can be tailored by changing the cooling rate. Equiaxed grain structure can be obtained by extensive deformation in the  $\alpha+\beta$  range followed by annealing at 700°C for 2 h and air cool (mill annealing) [36]. Ti6Al4V can be stress relieved by holding at 480-650°C for 1 to 4 h. Full stress relief is achieved after 50 h at 595°C, and 50 % of stresses are removed after about 1 h at 595°C [36]. Furnace cooling or air cooling from the stress relieving temperature are preferred [2]. Titanium alloys should be heat treated in atmospheres free of reducing gases and contaminants that can cause hydrogen pick up. Vacuum furnaces and protective gas furnaces are used to minimize contamination. [36]

Table 11. Nominal chemical composition of Ti6Al4V alloys. The values for N, C, H, Fe and O are impurity limits (max allowed). Values in wt%. [35]

	Al	V	N	C	H	Fe	O
Ti-6Al-4V	6	4	0.05	0.10	0.010-0.015	0.3	0.2
Ti-6Al-4V ELI (AMS 4907 and 4930)	5.5-6.75	3.5-4.5	0.05	0.08	0.0125	0.25	0.13

### Additive manufacturing

During the L-PBF manufacturing process the material is first brought to liquid state and when cooled below solidus temperature the  $\beta$ -phase begins to form and upon further cooling below  $\beta$  transus temperature  $\alpha/\alpha'$  phases form within the prior  $\beta$  grains. The thermal history during the process dictates the phase composition of the material and due to rapid cooling in the L-PBF process the as-built structure consist mostly of needle shaped  $\alpha'$  martensite formed within the prior  $\beta$  grains. [48] However it is possible to produce a  $\alpha + \beta$  dual phase structure using L-PBF by using low scanning speed and low laser power to lower the cooling rate allowing diffusion to take place [49]. The layered construction results in a columnar grain structure where the  $\beta$  grains extend over several layers due to epitaxial growth. For this reason,

the material is highly anisotropic in the as-built condition. The subsequent heating of already solidified layers during processing coarsens the grains. For tall builds, the top layers cool more slowly compared to the bottom layers because of the low thermal conductivity of Ti6Al4V, thus influencing the evolving microstructure. Ti-alloys are easily contaminated by oxygen, which adversely affects the mechanical properties, making careful handling of feedstock powder and build atmosphere to avoid oxygen contamination critical.

Thermal post processing guidance is provided in ASTM F2924-14 [50] for L-PBF manufactured Ti6Al4V and in ASTM F3001-14 [51] for Ti6Al4V ELI. Same guidance is also found in ASTM F3301-18 [39] for both alloys. The delivery conditions (heat treatments) specified in the standards are: 1) Stress relieved (SAE AMS2801 or SAE AMSH81200), 2) Annealed (SAE AMS2801 or SAE AMSH81200), 3) Solution annealing + ageing (AMS2801), 4) HIP and 5) All thermal post processing is optional.

L-PBF fabricated material typically has higher tensile, and yield strength compared to wrought alloy, but the ductility is lower. Stress relieving at temperatures  $\leq 800^{\circ}\text{C}$ , which is the typical practice, does not change the microstructure significantly and results in a slight increase in ductility. The yield and tensile strengths are highest in the as-built condition while the elongation is the lowest. [48] Since defects have a detrimental effect on fatigue properties, the HIP processing is commonly performed to reduce the porosity after printing. Yan X. et al. [52] investigated the effect of different thermal post processes on microstructure, tensile properties and fatigue performance of L-PBF manufactured Ti6Al4V ELI (EOS M290, EOS powder, layer thickness 50  $\mu\text{m}$ ). They conducted a HIP treatment in a vacuum furnace at  $900^{\circ}\text{C}$  for 2 h in 120 MPa, cooled the samples in furnace below  $200^{\circ}\text{C}$  and subsequently air cooled to room temperature (conforming to ASTM 2924-14), which transformed the  $\alpha'$  martensitic structure into a structure consisting of decomposed  $\alpha$  grains embedded in  $\beta$  grain boundaries. The HIP effectively removed the porosity, which was measured as  $<0.03\%$  in as-built condition. Based on EBSD analysis the amount of  $\beta$  phase before and after HIP was low, 5 % and 4 % respectively, while the rest consisted of  $\alpha$ -phase. The mechanical properties after HIP were; Tensile strength = 941 MPa, Yield strength = 839 MPa, Elongation at break = 19 %, Young's modulus = 115 GPa. The tensile properties after HIP treatment exceeded the minimum requirements in ASTM F2924-14. The authors observed that stress relief at  $900^{\circ}\text{C}$  produced a  $\alpha+\beta$  lamellar microstructure and had good mechanical properties with much higher ductility compared samples stress relieved at  $800^{\circ}\text{C}$ . The fatigue strength (axial test in build direction,  $f = 130\text{ Hz}$ ) improved after HIP compared to as-built samples, where fatigue strength after HIP at  $10^5$  cycles was approximately 500 MPa and the apparent endurance limit at  $10^7$  cycles was 370 MPa. According to Liang Z. et al. [53] the as-built structure consisting of  $\alpha'$  begins to transform into  $\alpha$  and  $\beta$  above  $760^{\circ}\text{C}$ . Water quenching from the solution anneal temperature of  $950^{\circ}\text{C}$  transforms the  $\beta$ -phase to  $\alpha'$  resulting in phase structure consisting of  $\alpha$  and  $\alpha'$ . Solution anneal at  $950^{\circ}\text{C}$  for 2 h (water quenched) followed by aging at  $540^{\circ}\text{C}$  for 4h (air cool) resulted in coarsened lamellar structure consisting of  $\alpha$  and  $\alpha'$  where some  $\beta$  was formed within the  $\alpha'$  during aging. The lamellar  $\alpha / \alpha'$  structure had lower strength and similar ductility compared to the fully acicular  $\alpha'$  structure of the as-built samples and samples heat treated at  $600^{\circ}\text{C}$ . Samples annealed at temperatures ranging from  $800^{\circ}\text{C}$  to  $900^{\circ}\text{C}$  had a  $\alpha + \beta$  structure consisting of  $\alpha$  lamella and irregular  $\beta$  resulting in higher elongation and lower strength compared to as-built samples. [53]

It is worth noting that the equiaxed (mill annealed) microstructure common for traditionally manufactured Ti6Al4V is not achievable using L-PBF technology, which produces a metastable anisotropic microstructure.

Table 12. Mechanical properties of Ti6Al4V.

	Ti6Al4V (Annelaet)1	Ti6Al4V (Solution treated + Aged)1	Ti6Al4V (low oxygen, Annealed)1	SLM Solutions, 30µm, vertical (As-built)2	SLM Solutions, 30µm, vertical (Heat treated)3	SLM Solutions, 30µm, vertical (HIP)4	EOS, vertical (As-built)5	EOS, vertical (Heat treated)6
Young's modulus [GPa]	113,8	-	113,8	117 ± 2	126 ± 1	124 ± 6	110 ± 15	110 ± 15
Yield strength [MPa]	830-924	1103	760-827	1170 ± 26	887 ± 12	935 ± 12	1120 ± 80	1000 ± 60
Tensile strength [MPa]	900-993	1172	830-896	1289 ± 17	960 ± 4	1002 ± 7	1240 ± 50	1100 ± 40
Elongation [%]	14	10	15	9 ± 1	14 ± 1	14 ± 1	10 ± 3	14,5 ± 2
Reduction of area [%]	30	25	35	29 ± 7	50 ± 2	41 ± 4		
Impact toughness [J]	14-19	-	24	11 ± 1	29 ± 3	23 ± 3		
Hardness	36 HRC	41 HRC	35 HRC	362 ± 11	307 ± 4	316 ± 10	320 ± 12 HV5	

<sup>1</sup> Minimum and average mechanical properties of wrought titanium alloys at room temperature. If a range is given, the lower value is a minimum, all other values are averages. [35]

<sup>2</sup> Vertical orientation. Layer thickness 30µm. Tensile test: ISO 6892-1:201. Hardness: DIN EN ISO 6507-1:2018. Charpy: DIN EN ISO 148-1:2017-05. [54]

<sup>3</sup> Vertical orientation. Layer thickness 30µm. Specimens were heated up in vacuum atmosphere at a rate of < 450 °C/h up to 910 °C, then with < 300 °C/h up to 940 °C. Subsequent holding at 940 ± 10 °C for 4 h -0/+30 min. Cooling down in vacuum at a rate of 40 ± 10 °C/h to 760 ± 15 °C, then in argon with 560 ± 100 °C/h to ≤ 480 °C, followed by gas fan quenching at any rate to ≤ 50 °C. [54]

<sup>4</sup> Vertical orientation. Layer thickness 30µm. Specimens were HIPed with 920 ± 10 °C and 1000 bar for 2 h. [54]

<sup>5</sup> Vertical orientation. EOS M280 / M290 (400W). Tensile testing according to ISO 6892-1:2009 (B) Annex D. Vicker hardness measurement according to: EN ISO 6507-1. [55]

<sup>6</sup> Vertical orientation. EOS M280 / M290 (400W). Specimens were treated at 800 °C (1470 °F) for 4 hours in argon inert atmosphere. [55]

## 6 Nickel-based superalloys

Superalloys are complex heat-resisting alloys based on nickel, nickel-iron or cobalt. They are used in gas turbines and other applications where heat and/or corrosion resistance are of paramount importance. Superalloys are generally used at temperatures above 540°C. The solubility of elements in nickel such as copper, iron, cobalt and chromium are high enabling great versatility in nickel alloys. The face-centered cubic (FCC) crystal structure of nickel (γ-phase) can be strengthened by solid-solution strengthening (Inconel 625), carbide precipitation and precipitation hardening (Inconel 718).

### 6.1 Inconel 625

Alloy 625 is a solid solution strengthened Ni-Cr-Mo alloy, which has excellent heat and corrosion resistance containing approximately 60 % Ni, 20 % Cr, 9 % Mo and small amounts

of other elements such as iron and niobium (Table 13). Alloy 625 has low amounts of precipitate forming elements such as aluminum and titanium. [35] The main strengthening comes from molybdenum and niobium additions, but some strength improvement may come from precipitation of carbides and/or intermetallic compounds although the alloy generally consists of austenitic  $\gamma$ -phase only. [56] The alloy is resistant to pitting and crevice corrosion, has high corrosion-fatigue strength, high tensile, creep and rupture strength and excellent fatigue strength including thermal fatigue. These properties make it suitable for marine applications where exposure to sea water is expected. Alloy 625 is typically used in chemical processing equipment, aircraft engine and airframe components, ship and submarine parts and nuclear reactors [56].

Alloy 625 is typically delivered in mill annealed condition for the purpose of restoring material properties after forming processes. Mill annealing results in fine grain size (recrystallization), which is beneficial for low-cycle fatigue strength. The alloy can be mill annealed by holding at 925°C for 5 - 20 min (thin sections) followed by rapid cooling. For hot worked material, the solution annealing procedure is more commonly applied. [2] Solution annealing provides maximum ductility, and typical solution anneal procedure for alloy 625 is to soak at 1150°C for 2 h and cool rapidly (rapid air cooled or water quenched) below 540°C to avoid precipitations [36]. The applicable solution annealing temperature range is 1095 - 1205°C [2].

Stress relieving can be performed below 650°C to avoid carbide precipitation, but the stress relieving effect diminishes at low temperatures. For full stress relief the mill anneal or solution anneal treatment is recommended. [56]

Table 13. Nominal chemical composition of Inconel 625 alloy. [56]

Element	Ni	Cr	Co	Mo	Nb	Al	Ti	Fe	Mn	Si	C
wt%	58.0	20.0- 23.0	1.0	8.0- 10.0	3.15- 4.15	0.40	0.40	5.0	0.50	0.50	0.10

### Additive manufacturing

Alloy 625 is versatile alloy designed for use in demanding corrosive high temperature environments and as such is important part of the L-PBF powder material portfolio. The rapid cooling rates during L-PBF create a fine cellular dendritic structure with segregation of alloying elements and a strong texture due to growth of grains along the build direction [57]. Also small equiaxed grains are typically observed, especially at the melt pool boundaries [57]. The solidification structure consists mainly of  $\gamma$ -phase but also contains precipitates such as  $\gamma'$ ,  $\gamma''$ , Laves and carbides. The choice of process parameters affect the forming microstructure, as laser parameters and scanning pattern can be tailored to increase texture and influence the phase structure of as-built material. [57]

Formation of non-equilibrium phases such as Laves phase are detrimental to the mechanical properties of superalloys and thermal post processing is therefore necessary to obtain desirable phase structure and good material properties. The thermal post processes (delivery conditions) specified in the AM standard ASTM F3056-14 [58] for Inconel 625 are stress relieved (AMS 2774), annealed (AMS 2774), and stress relieved (AMS 2774) + HIP (ASTM F3056-14) + annealed (AMS 2774). Marchese, G. et al. [59] studied the effect of different heat treatments (direct aging, solution anneal and solution anneal + aging) on the microstructure on mechanical properties of L-PBF manufactured Inconel 625 (EOS M270 machine, EOS powder, layer thickness = 20  $\mu\text{m}$ ). The as-built samples consisted of columnar grains with very fine dendritic / cellular structures, with the interdendritic regions containing nano-sized Nb-rich MC carbides and Nb, Mo rich areas. The authors did not observe Laves phase in the as-built microstructure. Direct aging at 700°C / 24 h did not alter the dendritic structure, but resulted in

precipitation of MC carbides at the grain boundaries as well as in inhomogeneous precipitation of  $\gamma''$  phase. Solution annealing at 1150°C for 2 h (water quenched) resulted in a recrystallized microstructure with equiaxed grain structure with twin boundaries, eliminating the prior dendritic structure. Growth of the primary MC carbides was observed along with precipitation of secondary carbides. Samples that were solution annealed and further aged at 700°C for 24 h had similar grain structure (shape/size) as the solution annealed samples, but with  $M_{23}C_6$  carbides at the grain boundaries and homogenous  $\gamma''$  intergranular precipitation. All samples except the ones directly aged after printing had tensile properties that exceeded the minimum values in ASTM F3056-14 standard. The directly aged samples had lower ductility than specified in the standard (23 % vs 30 %). Solution annealed and aged samples had the highest tensile strength ( $1116 \pm 6$  MPa) and elongation at break was  $35 \pm 5$  %, whereas the solution annealed samples had the lowest tensile strength ( $883 \pm 15$  MPa) and highest ductility (elongation at break =  $55 \pm 1$  %). The dendritic structure and high dislocation density of the as-built samples resulted in relatively good mechanical performance exhibiting mainly ductile fracture. The directly aged samples had the highest number of brittle fractures on the fracture surfaces, which the authors attributed to the presence of Nb-rich MC carbides,  $M_{23}C_6$  carbides and  $\gamma''$  phases. The fracture mechanism for the solution annealed samples was ductile while the solution annealed and aged samples had a mixture of ductile and brittle fracture due to the presence of  $M_{23}C_6$  carbides and  $\gamma''$  phase. [59]

The mechanical properties of L-PBF manufactured and stress relieved alloy 625 (EOS 270 machine, EOS IncodALLOY 625 powder) was investigated by Hack, H. et al. [60]. Stress relieving was performed in accordance with AMS 2774 (ASTM F3056-14) by heat treating tensile, Charpy-V, small/large compact tension (CT) specimens among other test samples at 1038°C followed by air cool. The samples were machined prior to testing. The tensile properties of the stress relieved samples exceeded the minimum values in ASTM F3056-14 except for two vertically built samples that had elongation values slightly below 30 %. Samples built horizontally had much higher ductility compared to vertically built tensile test specimens. The impact energies ranged from 94 to 149 J for horizontally oriented samples and from 131 to 150 J for vertically oriented samples, exceeding the minimum values for wrought plate. The fracture toughness for samples with crack propagation direction parallel and perpendicular to build direction were reported as 410.1 kJ/m<sup>2</sup> and 408.6 kJ/m<sup>2</sup>, respectively, which were considered as excellent values by the authors. The effect of HIP processing on the microstructure and mechanical properties on L-PBF manufactured (SLM Solutions 125 HL system, SLM Solutions power, layer thickness = 30µm, in-house parameters) Inconel 625 was reported by Gonzalez, J. A., et al [61]. Tensile test specimen were HIP'd at 1163°C  $\pm$  3.5 °C for 3 h in 102 MPa  $\pm$  1.72 MPa atmosphere and subsequently machined. Both the as-built and HIP'd samples had an apparent density of 99.9 %. After HIP the parts had an equiaxed grain structure with average grain size of 27 µm. The mechanical properties of HIP processed samples well exceeded the minimum values specified in ASTM F3056-14. The vertically oriented samples had higher tensile strength, yield strength and elongation at break than the horizontally oriented samples. Fracture surface analysis revealed dimples on the fracture surface indicating a ductile fracture. The mechanical properties of wrought and L-PBF manufactured Inconel 625 are presented in Table 14.

Table 14. Mechanical properties of wrought and AM Inconel 625 alloy.

	625 (wrought and annealed) <sup>1</sup>	SLM Solutions, 30µm, vertical (As-built) <sup>2</sup>	SLM Solutions, 30µm, vertical (Annealed) <sup>3</sup>	EOS, 40µm, vertical (As-built) <sup>4</sup>	EOS, 40µm, vertical (Annealed) <sup>5</sup>
Young's modulus [GPa]	207	153 ± 18	190 ± 9	-	
Yield strength [MPa]	517	686 ± 11	646 ± 4	630 ± 5	640 ± 5
Tensile strength [MPa]	930	945 ± 10	938 ± 7	870 ± 10	890 ± 10
Elongation (%)	42.5	42 ± 5	45 ± 1	48 ± 2	49 ± 2
Reduction of area [%]	-	44 ± 8	49 ± 3	-	-
Impact toughness [J]	-	-	-	-	-
Hardness	190 HB	303 ± 7 HV10	297 ± 4 HV10	-	-

<sup>1</sup> Properties are for annealed sheet unless otherwise indicated. [56]

<sup>2</sup> Vertical orientation. Layer thickness 30µm. Tensile test: ISO 6892-1:201. Hardness: DIN EN ISO 6507-1:2018. [62]

<sup>3</sup> Vertical orientation. Layer thickness 30µm. Specimens were heated up to 870 °C with subsequent holding for 1 h, followed by air-cooling. According to AMS 5599. Tensile test: ISO 6892-1:201. Hardness: DIN EN ISO 6507-1:2018. [62]

<sup>4</sup> Vertical orientation. Layer thickness 40µm. Tensile testing according to ISO 6892-1 B10, proportional test pieces. [55]

<sup>5</sup> Vertical orientation. Layer thickness 40µm. Heat treatment procedure: anneal at 870 °C (1600 °F) for 1 hour, rapid cooling. Tensile testing according to ISO 6892-1 B10, proportional test pieces. [55]

## 6.2 Inconel 718

Inconel 718 is a precipitation-hardening alloy and as such, more complex alloy in terms of post processing compared to solution-strengthened alloys. High strength and corrosion resistance at high temperatures have made Inconel 718 the most popular nickel-base superalloy used in industrial applications [56]. The alloy has high strength and corrosion resistance at temperatures reaching 700°C and is widely used in aircraft turbine engines, airframe parts, bolts and fasteners, oil & gas industry as well as in nuclear industry [56]. Inconel 718 contains large amounts of iron, niobium and molybdenum and lesser amounts of aluminum and titanium (Table 15). [35]

Table 15. Nominal chemical composition of wrought Inconel 718. [35]

Element	Ni	Cr	Co	Mo	Nb	Al	Ti	Fe	Mn	Si	C	B	Other
wt%	50-55	17.0-21.0	1.0	2.80-2.30	4.75-5.50	0.20-0.80	0.65-1.15	balance	0.35	0.35	0.08	0.006	0.3 Cu

Aside from the solution strengthening effect the alloy obtains its excellent mechanical properties mainly from the FCC  $\gamma'$  ( $\text{Ni}_3\text{Al,Ti}$ ) and especially the BCT  $\gamma''$  ( $\text{Ni}_3\text{Nb}$ ) precipitates as well as from carbides [56]. The  $\gamma'$  precipitates uniformly in the  $\gamma$  matrix providing high-temperature strength and creep resistance. The  $\gamma''$  is the primary strengthening phase in Inconel 718 with much higher volume fraction than  $\gamma'$  providing high strength at low to intermediate temperatures. [1] However, the metastable  $\gamma''$  begins to transform into detrimental phases at sufficient exposure times to temperatures exceeding 650°C resulting in sharp reduction in strength, which is why the maximum service temperature in practice is  $\leq$



650°C [56]. At sufficiently high temperatures phases such as Laves,  $\delta$  and  $\sigma$  can form that are detrimental to the material properties.

The alloy is typically used in solution annealed and aged condition and the mechanical properties can be tailored by altering the heat treatment temperatures, hold times and cooling rates [2]. Wrought Inconel 718 can be directly aged by quenching the alloy after forging and performing a two-step aging treatment. For solution treatment, temperature range of 925 - 1010°C and hold times of 1 - 2 h are typically used followed by cooling at rates higher or equal to air cool. Aging is done in two steps by first ageing at 720°C for 8 h, then cooling in the furnace to 620°C and holding for 18 h and subsequently air cooled. Higher solution treatment temperatures (1040°C to 1065°C) and longer ageing hold times can be used to increase ductility, impact properties and low temperature toughness with the risk of notch brittleness in stress rupture [2]. Cast Inconel 718 parts are produced by investment casting [2], which tends to create porosity in the as-cast structure. HIP processing is often employed to remove the porosity, which is critical especially for aerospace components. The HIP process is typically done near the solution temperatures under inert gas atmosphere. Rapid cooling is preferred but in some cases a separate high temperature anneal followed by rapid cool is required. Large sections can be homogenized prior to HIP processing to increase local melting temperature. [2] After HIP the parts are subject to solution anneal / homogenization and aging treatments [63].

#### *Additive manufacturing*

Inconel 718 is challenging to process into complex forms and machine, making it an attractive material for AM technologies. Similarly to Inconel 625, the L-PBF processed Inconel 718 typically has a cellular  $\gamma$  sub-structure with micro-segregation and elongated grains typically oriented parallel to the build direction  $\langle 001 \rangle$ , thus having strong texture. [63] The presence of Laves phase in as-built alloy has also been reported [64]. The cooling rates decrease as the built height increases resulting in coarsening of the grains. Generally, lower linear densities (laser power divided by scanning speed) lead to lesser micro-segregation and changes in the precipitation kinetics during ageing. However, too low linear densities lead to increased porosity. [64]

The inhomogeneous microstructure and the insufficient precipitation of the strengthening phases in as-built Inconel 718 necessitate the use of post heat treatments to achieve desirable mechanical properties. Thermal post treatments for LBPf manufactured Inconel 718 are specified in the ASTM F3055-14a standard [65], including the following heat treatment procedures: 1) Stress relieving, 2) Solution treatment + ageing in accordance with AMS 2774 and 3) HIP. The recommended solution treatment temperatures in AMS 2774 depend on product types ranging from 954°C to 1066°C [30]. The purpose of solution treatment is to dissolve the unwanted phases into solution and to homogenize the material for uniform precipitation of the  $\gamma'$  and  $\gamma''$  phases during the ageing process. [63]

According to Tucho, W.M et al. [66] the temperature of 980°C is not sufficiently high for solution annealing of L-BPF built Inconel 718 as Laves and micro-segregates are not completely dissolved. Solution annealing at 1100°C for 1 h resulted in partial recrystallization but did not fully dissolve the precipitates whereas longer hold time (7 h) resulted in complete recrystallization, grain coarsening and the dissolving of Laves and other unwanted phases. At 1250°C the microstructure was fully recrystallized (coarse grained) and homogenous. [66]

Xu et al. [67] studied the microstructure and creep performance of L-PBF manufactured Inconel 718 after different post heat treatments. Heat treatment that is specified in AMS 5383 standard for cast Inconel 718 (homogenization at 1093°C + solution treatment at 954–982 °C + ageing at 718 °C and 620 °C) transformed the anisotropic as-built structure into equiaxed grain structure. Similar microstructure was observed for samples HIP'd at 1200°C for 4 h in

103 MPa, expect for the amount of precipitates that was significantly higher for the HIP'd specimen. The HIP'd specimens had pronounced intergranular cracking under creep conditions which the authors attributed to the intergranular precipitations. [67] Aydinöz, M.E. et al. [64] reported similar findings regarding the microstructure of HIP'd Inconel 718, as  $\delta$  precipitates were observed at grain boundaries resulting in lower strength compared to solution aged and aged samples. The HIP parameters used in literature range from 100 to 200 MPa for gas pressure and 1150 to 1280°C for temperature, where temperatures below 1200°C are most common to prevent excessive grain growth [63].

Gallmayer, T.G. et al. [68] investigated the effect of various heat treatments on the microstructure and mechanical properties of Inconel 718. The different heat treatments they performed included solution anneal (980°C / 1 h / air cool) + aging (720°C / 8 h + 620°C / 8 h + air cool), direct aging at different temperatures and solution annealing (1020°C / 0.25 h / water quench) + aging (720°C / 24 h / air cool). The standard practice, i.e. solution treatment at 980°C and aging (AMS 5662), produces mechanical properties on par with wrought Inconel 718 but not optimal in terms of composition and size of precipitates. The detrimental Laves and  $\delta$  phases were reportedly not found in the sample solution annealed at 1020°C. The authors stated that the AM process induces dislocation cells and nano-sized precipitates in the microstructure providing strength, elongation and creep performance that are retained if solution temperatures below 1100°C are used. However, solution annealing above 1010°C is sufficient to eliminate  $\delta$  and Laves phase. Therefore the solution anneal step was seen essential and rapid cooling from solution annealing temperatures below 720°C was recommended, but the two-step aging procedure was not, as optimal precipitate structure ( $\gamma'$ ,  $\gamma''$ ) was observed after single aging step at 720°C. [68]

According to published research, the fatigue performance of L-PBF manufactured Inconel 718 is inferior to wrought or even cast counterparts, which is more evident in the long-life regime. Comparable fatigue properties to wrought material have been obtained after HIP as long as the effect of surface roughness is eliminated [63]. The mechanical properties of wrought, cast and AM Inconel 718 are shown in Table 16.

Table 16. Mechanical properties of Inconel 718.

	Wrought 718 (Solution anneal + aging) <sup>1</sup>	Wrought 718 (Solution anneal + aging) <sup>2</sup>	SLM Solutions, 30 $\mu$ m, vertical (As-built) <sup>3</sup>	SLM Solutions, 30 $\mu$ m, vertical (Solution anneal + aging) <sup>4</sup>	EOS, 40 $\mu$ m, vertical (As-built) <sup>5</sup>	EOS, 40 $\mu$ m, vertical (Solution anneal + aging) <sup>6</sup>
Young's modulus [GPa]	-	-	168 $\pm$ 10	186 $\pm$ 15	-	-
Yield strength [MPa]	1130	1255	684 $\pm$ 6	1225 $\pm$ 68	800	1240
Tensile strength [MPa]	1330	1415	1027 $\pm$ 10	1412 $\pm$ 86	1090	1505
Elongation [%]	23	17	29 $\pm$ 5	11 $\pm$ 5	25	12
Reduction of area [%]	48	41	40 $\pm$ 5	25 $\pm$ 6	-	-
Impact toughness [J]	-	-	80 $\pm$ 8	28 $\pm$ 3	-	-
Hardness	48 HRC	41 HRC	303 $\pm$ 7 HV10	470 $\pm$ 4 HV10	-	47 HRC / 466 HB
Fracture toughness $J_{1c}$ [MPa $\cdot$ m <sup>1/2</sup> ]	100	84	-	-	-	-

<sup>1</sup> Solution anneal: 955°C for 2 h, water quench or air cool; Age: 720°C for 8 h, cool 55°C/h to 620°C, hold 8 h, air cool. [2]

<sup>2</sup> Solution anneal: 1050°C for 1 h, air cool; Age: 760°C for 6 h, furnace cool 55°C/h to 650 °C, hold 8 h, air cool [2]

<sup>3</sup> Vertical orientation. Layer thickness 30µm. Tensile test: ISO 6892-1:2017. Hardness: DIN EN ISO 6507-1:2018. [69]

<sup>4</sup> Vertical orientation. Layer thickness 30µm. Specimens were heated up to 980 °C in a furnace, held for 1 h, followed by air-cooling + heating up to 720 °C, hold for 8 h, then cool down to 620 °C in furnace with 50 °C/h. Hold at 620 °C for 8 h, then air-cooling. Tensile test: ISO 6892-1:2017. Hardness: DIN EN ISO 6507-1:2018. [69]

<sup>5</sup> Vertical orientation. Layer thickness 40µm. Number of samples = 36. [70]

<sup>6</sup> Vertical orientation. Layer thickness 40µm. Heat treatment procedure conform to Aerospace Material Specification AMS 2774 and AMS 5662 (solution anneal at 954°C / 1h per 25mm, air cool + aging at 718°C / 8h + 621°C / 18h, air cool). Number of samples = 26. [70]

## 7 Summary

Relevant observations derived from the reviewed literature regarding heat treatment of AM alloys are summarized in Table 17.

Table 17. Summary of heat treatments for AM alloys based on the reviewed literature.

Alloy	Thermal post processing guidance in ASTM standard	Typical heat treatment	Microstructure after heat treatment (conventional)	Heat treatment considerations for AM alloy	AM microstructure	Mechanical properties
316L	yes (ASTM F3184-16)	Annealing	Austenitic, equiaxed	Heat treatment above 900°C is required for maximum stress relief. Solution annealing typically does not result in homogenous microstructure but rather coarsening of as-built grain structure or partial recrystallisation. HIP as per ASTM F3184-16 produces recrystallised structure.	AM microstructure is anisotropic with elongated grains, fine dendrites and microsegregation. Annealing results in grain growth and partial recovery. HIP results in partial or full recrystallisation. Oxide inclusions tend to grow during heat treatments.	AM alloy has its highest strength in the as-built condition (superior to wrought alloy). Tensile properties are comparable/ superior to wrought alloy in annealed/ HIP'd condition. Impact toughness is lower than that of wrought alloy.
Maraging	no	Solution anneal & age hardening	Martensite & second phase precipitates (Ni3Mo, Ni3Ti)	Conventional heat treatment procedure is sufficient for AM alloy: Solution anneal at 820°C followed by ageing at 460-480°C. Higher aging temperatures can be used for improved ductility and lower strength.	Mostly martensitic with some retained austenite. The texture present in the as-built material is reduced after annealing.	Strength increases with annealing and aging heat treatments and is comparable to conventional age-hardened maraging.
17-4 PH	no	Solution treatment & aging	Martensite (lath) & second phase precipitates	Solution annealing at ~1040°C and ageing at ~480°C (H900) can be considered an effective heat treatment procedure for the AM alloy.	Fine martensitic grain structure after solution anneal and ageing. As-built material has some retained austenite. High nitrogen concentration in feedstock powder can increase the fraction of retained austenite.	Tensile properties comparable to wrought alloy can be obtained for AM alloy by using appropriate solution annealing and ageing parameters. Some anisotropy between samples built in different orientations is likely to remain after heat treatments.

Alloy	Thermal post processing guidance in ASTM standard	Typical heat treatment	Microstructure after heat treatment (conventional)	Heat treatment considerations for AM alloy	AM microstructure	Mechanical properties
H13	no	Hardening & double tempering	Tempered martensite, & vanadium carbides	Quenching (1020°C, AC) and double tempering (~600°C) results in high strength but low ductility. HIP (1130°C / 6 h, 100MPa) performed prior to quenching and tempering improves ductility and strength.	The microstructure after hardening and double tempering consists of tempered martensite with some retained austenite and relatively homogenous precipitation of fine secondary carbides. Heat treatment at austenite temperature removes the cellular/dendritic solidification structure.	Quenched and double tempered alloy has comparable/ superior strength and lower ductility than wrought alloy.
AlSi10Mg	yes (ASTM F3318 - 18)	T6: Solution treatment & artificial aging	$\alpha$ (Al) + Si dendritic structure, Mg <sub>2</sub> Si precipitates	Solution treatment temperature above 480°C is recommended to produce a homogenous solid solution. The growth of hydrogen porosity has been reported at temperatures >525°C. Ageing temperatures between 160-180°C have been utilised effectively, but the hold times have to be adjusted accordingly.	Solution annealing leads to coarsening of Al-rich cellular grains and Si-particles surrounding the grains. Artificial ageing leads to precipitation of Mg <sub>2</sub> Si.	Solution-treated and aged AM alloy has similar strength as a cast- and heat-treated alloy (T6) but has higher ductility.
Ti6Al4V	yes (ASTM F2924 - 14, ASTM F3001 - 14)	Solution treatment & aging	$\alpha$ + transformed $\beta$	Stress relief at 900°C was recommended over the lower temperatures as it produced $\alpha$ + $\beta$ lamellar structure with good mechanical properties. The traditional solution annealing + ageing process does not necessarily produce optimal microstructure for AM alloys but is still applicable in terms of tensile properties. HIP processing in accordance with ASTM F2924-14 produced a structure with $\alpha$ grains embedded in $\beta$ grain boundaries.	Fully martensitic $\alpha'$ structure within prior $\beta$ grains in the as-built condition. Annealing produces a lamellar $\alpha$ + $\beta$ structure. Quenching from solution anneal temperature transforms $\beta$ into $\alpha'$ . Some $\beta$ forms during ageing heat treatment.	The as-built material with acicular $\alpha'$ structure has the highest strength, which is superior to a wrought and annealed alloy, but has lower ductility. Annealing improves ductility due to formation of a + $\beta$ structure with a decrease in strength. Solution-treated and aged material has slightly lower strength than a wrought and heat-treated alloy. HIP processing improves ductility and fatigue strength more effectively than the as-built condition.
Inconel 625	yes (ASTM F3056 - 14e1)	Solution anneal	Austenitic (solution strengthened)	The typical solution annealing at 1150°C followed by a water quench produced a ductile recrystallised structure. Ageing increases strength	Equiaxed recrystallised grain structure after solution annealing and quenching. Primary MC carbides	As-built material has higher strength and ductility comparable to wrought and annealed alloy. Slight improvement in mechanical

Alloy	Thermal post processing guidance in ASTM standard	Typical heat treatment	Microstructure after heat treatment (conventional)	Heat treatment considerations for AM alloy	AM microstructure	Mechanical properties
				but reduces ductility due to precipitations.	and secondary carbides.	properties are achievable via an appropriate solution-annealing process.
Inconel 718	yes (ASTM F3055 - 14a)	Solution anneal & aging	Austenitic with $\gamma'$ & $\gamma''$ precipitates (+ carbides)	The solution-annealing temperature should be above 980°C to dissolve second phases. Solution treatment temperature 1020°C has been proven effective. A single ageing step at 720°C is potentially more effective than the traditional two-step aging treatment. HIP at 1200°C resulted in precipitation of $\delta$ at grain boundaries.	Solution anneal at sufficient temperature results in a recrystallised equiaxed microstructure. Typical ageing procedure was found to be suboptimal for AM alloy in terms of $\gamma'/\gamma''$ phase structure. HIP can produce intergranular precipitations that are detrimental to mechanical properties.	The tensile properties of solution-annealed and aged AM alloy are comparable to a wrought and heat-treated alloy. HIP can result in precipitation of the $\delta$ phase, decreasing the strength of the material.

## 8 Conclusions

The conventional processing methods for producing castings, wrought and PM products are very different from the process conditions involved in the L-PBF process. Melting layers of powder produces highly anisotropic microstructures characterized by high dislocation density and microsegregation of elements among other phenomena due to the high solidification rates, remelting / reheating of previous layers and other process characteristics related to L-PBF.

For some alloys the as-built microstructure provides superior tensile properties compared to wrought or heat treated AM alloy, but is not necessarily ideal condition for all end use applications as other properties may be impaired. The heat treatment specifications found in the AM standards do not take into account the variation in process conditions, i.e. different machines, process parameters, that can influence on the finished material properties after heat treatment considerably. Attention should be paid to the feedstock material composition, especially to the amount of impurity elements.

The heat treatment guidance for AM alloys is largely based on aerospace specifications that are not designed for the L-PBF process. According to the reviewed literature the traditional heat treatment procedures can result in satisfactory mechanical properties and even superior performance compared to wrought / cast alloys and in some instances a modification to the practices are found to improve the material performance. However, often the microstructure and the material properties are different for AM parts after heat treatment compared to conventionally manufactured parts which demonstrates a need to develop heat treatment practices specifically for AM alloys and to adopt and modify the existing practices to better suit the L-PBF process.

## References

---

- [1] ASM International Handbook Committee, *ASM Handbook Vol. 1: Properties and Selection: Irons, Steels, and High-Performance Alloys*. 1990.
- [2] ASM International Handbook Committee, *ASM Handbook Vol. 4: Heat Treating*. 1991.
- [3] H. Chandler, *Heat Treater's Guide - Practices and Procedures for Irons and Steels (2nd Edition)*. ASM International, 1995.
- [4] ASTM International, "ASTM F3184 (2016) Standard Specification for Additive Manufacturing Stainless Steel Alloy (UNS S31603) with Powder Bed Fusion," *Annual Book of ASTM Standards*. West Conshohocken, PA 19428-2959, United States, pp. 1–9, 2016.
- [5] A. B. Kale, J. Singh, B.-K. Kim, D.-I. Kim, and S.-H. Choi, "Effect of initial microstructure on the deformation heterogeneities of 316L stainless steels fabricated by selective laser melting processing," *J. Mater. Res. Technol.*, vol. 9, no. 4, pp. 8867–8883, 2020, doi: 10.1016/j.jmrt.2020.06.015.
- [6] T. Larimian, M. Kannan, D. Grzesiak, B. AlMangour, and T. Borkar, "Effect of energy density and scanning strategy on densification, microstructure and mechanical properties of 316L stainless steel processed via selective laser melting," *Mater. Sci. Eng. A*, vol. 770, no. September 2019, p. 138455, 2020, doi: 10.1016/j.msea.2019.138455.
- [7] A. Leicht, C. H. Yu, V. Luzin, U. Klement, and E. Hryha, "Effect of scan rotation on the microstructure development and mechanical properties of 316L parts produced by laser powder bed fusion," *Mater. Charact.*, vol. 163, no. December 2019, pp. 2–10, 2020, doi: 10.1016/j.matchar.2020.110309.
- [8] R. B. Rebak and X. Lou, "Environmental Cracking and Irradiation Resistant Stainless Steels by Additive Manufacturing," *Bonisteel Blvd.* pp. 1–98, 2018, doi: 10.2172/1431212.
- [9] X. Lou, P. L. Andresen, and R. B. Rebak, "Oxide inclusions in laser additive manufactured stainless steel and their effects on impact toughness and stress corrosion cracking behavior," *J. Nucl. Mater.*, vol. 499, 2018, doi: 10.1016/j.jnucmat.2017.11.036.
- [10] A. Puichaud *et al.*, "Microstructure and mechanical properties relationship of additively manufactured 316L stainless steel by selective laser melting To cite this version : HAL Id : cea-02458434 Microstructure and mechanical properties relationship of additively manufactured ," 2020.
- [11] N. P. Lavery *et al.*, "Effects of hot isostatic pressing on the elastic modulus and tensile properties of 316L parts made by powder bed laser fusion," *Mater. Sci. Eng. A*, vol. 693, no. March, pp. 186–213, 2017, doi: 10.1016/j.msea.2017.03.100.
- [12] A. J. Cooper, N. I. Cooper, J. Dhers, and A. H. Sherry, "Effect of Oxygen Content Upon the Microstructural and Mechanical Properties of Type 316L Austenitic Stainless Steel Manufactured by Hot Isostatic Pressing," *Metall. Mater. Trans. A*, vol. 47, no. 9, pp. 4467–4475, 2016, doi: 10.1007/s11661-016-3612-6.
- [13] MatWeb material data base, "Matweb material data: AISI Type 316L Stainless Steel, annealed and cold drawn bar." [Online]. Available: <http://www.matweb.com/search/DataSheet.aspx?MatGUID=c02b8c0ae42e459a872553e0ebfab648&ckck=1>. [Accessed: 02-Jul-2020].
- [14] SLM Solutions Group AG, "Material Data Sheet: Stainless Steel 316L / 1.4404 / A276," 2019. [Online]. Available: <https://www.slm-solutions.com/en/products/accessories-consumables/slmr-metal-powder/>. [Accessed: 01-Jul-2020].
- [15] EOS GmbH, "Material data sheet: EOS StainlessSteel 316L, M290," 2017. [Online]. Available: <https://www.eos.info/en/additive-manufacturing/3d-printing-metal/dmls-metal-materials>. [Accessed: 01-Jul-2020].
- [16] EOS GmbH, "Material data sheet: EOS MaragingSteel MS1," 2017. [Online]. Available: <https://www.eos.info/en/additive-manufacturing/3d-printing-metal/dmls-metal-materials>. [Accessed: 01-Jul-2020].

- [17] Z. C. Oter, Y. Gencer, and M. Tarakci, "Microstructure evolution and surface quality of laser-sintered maraging steel parts produced on different building platform positions," *Optik (Stuttg.)*, vol. 202, no. July 2019, p. 163568, 2020, doi: 10.1016/j.ijleo.2019.163568.
- [18] J. Mutua, S. Nakata, T. Onda, and Z. C. Chen, "Optimization of selective laser melting parameters and influence of post heat treatment on microstructure and mechanical properties of maraging steel," *Mater. Des.*, vol. 139, pp. 486–497, 2018, doi: 10.1016/j.matdes.2017.11.042.
- [19] B. Mooney, K. I. Kourousis, and R. Raghavendra, "Plastic anisotropy of additively manufactured maraging steel: Influence of the build orientation and heat treatments," *Addit. Manuf.*, vol. 25, no. July 2018, pp. 19–31, 2019, doi: 10.1016/j.addma.2018.10.032.
- [20] SLM Solutions Group AG, "Material Data Sheet: Tool Steel 1.2709 / A646 / M300," 2020. [Online]. Available: <https://www.slm-solutions.com/en/products/accessories-consumables/slmr-metal-powder/>. [Accessed: 01-Jun-2020].
- [21] EOS GmbH, "Material Data Sheet: EOS ToolSteel 1.2709," 2020. [Online]. Available: <https://www.eos.info/en/additive-manufacturing/3d-printing-metal/dmls-metal-materials>. [Accessed: 01-Jul-2020].
- [22] D. C. Ludwigson and A. M. Hall, "The Physical Metallurgy of Precipitation-hardenable Stainless Steels," Defence Metals Information Center, 1959.
- [23] H. K. Rafi, D. Pal, N. Patil, T. L. Starr, and B. E. Stucker, "Microstructure and Mechanical Behavior of 17-4 Precipitation Hardenable Steel Processed by Selective Laser Melting," *J. Mater. Eng. Perform.*, vol. 23, no. 12, pp. 4421–4428, 2014, doi: 10.1007/s11665-014-1226-y.
- [24] L. E. Murr *et al.*, "Microstructures and properties of 17-4 PH stainless steel fabricated by selective laser melting," *J. Mater. Res. Technol.*, vol. 1, no. 3, pp. 167–177, 2012, doi: 10.1016/S2238-7854(12)70029-7.
- [25] S. D. Meredith, J. S. Zuback, J. S. Keist, and T. A. Palmer, "Impact of composition on the heat treatment response of additively manufactured 17–4 PH grade stainless steel," *Mater. Sci. Eng. A*, vol. 738, no. July, pp. 44–56, 2018, doi: 10.1016/j.msea.2018.09.066.
- [26] Y. Sun, R. J. Hebert, and M. Aindow, "Effect of heat treatments on microstructural evolution of additively manufactured and wrought 17-4PH stainless steel," *Mater. Des.*, vol. 156, pp. 429–440, 2018, doi: 10.1016/j.matdes.2018.07.015.
- [27] M. Mahmoudi, A. Elwany, A. Yadollahi, S. M. Thompson, L. Bian, and N. Shamsaei, "Mechanical properties and microstructural characterization of selective laser melted 17-4 PH stainless steel," *Rapid Prototyp. J.*, vol. 23, no. 2, pp. 280–294, 2017, doi: 10.1108/RPJ-12-2015-0192.
- [28] SLM Solutions Group AG, "Material Data Sheet: Stainless Steel 17-4PH / 1.4542 / A564," 2019. [Online]. Available: <https://www.slm-solutions.com/en/products/accessories-consumables/slmr-metal-powder/>. [Accessed: 10-Jun-2020].
- [29] EOS GmbH, "Material data sheet: EOS StainlessSteel 17-4PH," 2017. [Online]. Available: <https://www.eos.info/en/additive-manufacturing/3d-printing-metal/dmls-metal-materials>. [Accessed: 01-Jul-2020].
- [30] F. Deirmina, N. Peghini, B. AlMangour, D. Grzesiak, and M. Pellizzari, "Heat treatment and properties of a hot work tool steel fabricated by additive manufacturing," *Mater. Sci. Eng. A*, 2019, doi: 10.1016/j.msea.2019.03.027.
- [31] M. Narvan, K. S. Al-Rubaie, and M. Elbestawi, "Process-Structure-Property Relationships of AISI H13 Tool Steel Processed with Selective Laser Melting," *Materials (Basel)*, vol. 12, no. 14, p. 2284, 2019, doi: 10.3390/ma12142284.
- [32] M. Åsberg, G. Fredriksson, S. Hatami, W. Fredriksson, and P. Krakhmalev, "Influence of post treatment on microstructure, porosity and mechanical properties of additive manufactured H13 tool steel," *Mater. Sci. Eng. A*, vol. 742, no. January 2018, pp. 584–589, 2019, doi: 10.1016/j.msea.2018.08.046.

- [33] ASTM International, "Standard Specification for Aluminum-Alloy Sand Castings." United States, 2003.
- [34] J. R. Davis, "Principles of Alloying \*," *Alloy. Underst. Basics*, 2001, doi: 10.1361/autb2001p003.
- [35] ASM International Handbook Committee, *ASM Handbook Vol. 2: Properties and selection--nonferrous alloys and special-purpose materials*. 1990.
- [36] H. Chandler, *Heat Treater's Guide - Practices and Procedures for Nonferrous Alloys*. ASM International, 1996.
- [37] CEN/TC 132 "Aluminium and aluminium alloys," "SFS-EN 1706 - Aluminium and aluminium alloys. Castings. Chemical composition and mechanical properties." Finnish Standards Association (SFS), Finland, 2010.
- [38] ASTM International, "ASTM F3318-18 - Standard for Additive Manufacturing – Finished Part Properties – Specification for AlSi10Mg with Powder Bed Fusion – Laser Beam," *ASTM Standards*. United States, 2018, doi: 10.1520/F3318-18.
- [39] ASTM International, "F3301 – 18a - Standard for Additive Manufacturing – Post Processing Methods – Standard Specification for Thermal Post-Processing Metal Parts Made Via Powder Bed Fusion," *ASTM Standards*. pp. 4–6, 2018, doi: 10.1520/F3301-18.
- [40] A. Sarentica, "Conventional heat treatment of additively manufactured AlSi10Mg," 2019.
- [41] E. A. Jäggle *et al.*, "Precipitation Reactions in Age-Hardenable Alloys During Laser Additive Manufacturing," *Jom*, vol. 68, no. 3, pp. 943–949, 2016, doi: 10.1007/s11837-015-1764-2.
- [42] Z. Li, Z. Li, Z. Tan, D. B. Xiong, and Q. Guo, "Stress relaxation and the cellular structure-dependence of plastic deformation in additively manufactured AlSi10Mg alloys," *Int. J. Plast.*, vol. 127, no. December 2019, p. 102640, 2020, doi: 10.1016/j.ijplas.2019.12.003.
- [43] L. Girelli, M. Tocci, M. Gelfi, and A. Pola, "Study of heat treatment parameters for additively manufactured AlSi10Mg in comparison with corresponding cast alloy," *Mater. Sci. Eng. A*, vol. 739, no. October 2018, pp. 317–328, 2019, doi: 10.1016/j.msea.2018.10.026.
- [44] C. Weingarten, D. Buchbinder, N. Pirch, W. Meiners, K. Wissenbach, and R. Poprawe, "Formation and reduction of hydrogen porosity during selective laser melting of AlSi10Mg," *J. Mater. Process. Technol.*, vol. 221, pp. 112–120, 2015, doi: 10.1016/j.jmatprotec.2015.02.013.
- [45] X. Garmendia, S. Chalker, M. Bilton, C. J. Sutcliffe, and P. R. Chalker, "Microstructure and mechanical properties of Cu-modified AlSi10Mg fabricated by Laser-Powder Bed Fusion," *Materialia*, vol. 9, no. January, p. 100590, 2020, doi: 10.1016/j.mtla.2020.100590.
- [46] SLM Solutions Group AG, "Material Data Sheet: Al-Alloy AlSi10Mg / EN AC-4300 / EN AC-AlSi10Mg," 2019. [Online]. Available: <https://www.slm-solutions.com/en/products/accessories-consumables/slmr-metal-powder/>. [Accessed: 08-Jun-2020].
- [47] EOS GmbH, "Material data sheet: FlexLine EOS, EOS Aluminium AlSi10Mg," 2018. [Online]. Available: <https://www.eos.info/en/additive-manufacturing/3d-printing-metal/dmls-metal-materials>. [Accessed: 01-Jul-2020].
- [48] S. Liu and Y. C. Shin, "Additive manufacturing of Ti6Al4V alloy: A review," *Mater. Des.*, vol. 164, p. 107552, 2019, doi: 10.1016/j.matdes.2018.107552.
- [49] M. Simonelli, Y. Y. Tse, and C. Tuck, "The formation of  $\alpha + \beta$  microstructure in as-fabricated selective laser melting of Ti-6Al-4V," *J. Mater. Res.*, vol. 29, no. 17, pp. 2028–2035, Sep. 2014, doi: 10.1557/jmr.2014.166.
- [50] ASTM International, "ASTM F2924 - 14 - Standard Specification for Additive Manufacturing Titanium-6 Aluminum-4 Vanadium with Powder Bed Fusion," *ASTM Standards*. United States, 2014, doi: 10.1520/F2924-14.
- [51] ASTM International, "ASTM F3001 - 14 - Standard Specification for Additive Manufacturing Titanium-6 Aluminum-4 Vanadium ELI (Extra Low Interstitial) with Powder Bed Fusion," *ASTM Standards*. United States, 2014, doi: 10.1520/F3001-14.



- [52] X. Yan *et al.*, "Effect of heat treatment on the phase transformation and mechanical properties of Ti6Al4V fabricated by selective laser melting," *J. Alloys Compd.*, vol. 764, pp. 1056–1071, 2018, doi: 10.1016/j.jallcom.2018.06.076.
- [53] Z. Liang, Z. Sun, W. Zhang, S. Wu, and H. Chang, "The effect of heat treatment on microstructure evolution and tensile properties of selective laser melted Ti6Al4V alloy," *J. Alloys Compd.*, vol. 782, pp. 1041–1048, 2019, doi: 10.1016/j.jallcom.2018.12.051.
- [54] SLM Solutions Group AG, "Material Data Sheet: Ti-Alloy TiAl6V4 ELI (Grade 23) / 3.7165 / B348 / F136," 2019. [Online]. Available: <https://www.slm-solutions.com/en/products/accessories-consumables/slmr-metal-powder/>. [Accessed: 29-Jun-2020].
- [55] EOS GmbH, "Material data sheet: EOS NickelAlloy IN625 EOS," 2017. [Online]. Available: <https://www.eos.info/en/additive-manufacturing/3d-printing-metal/dmls-metal-materials>. [Accessed: 01-Jul-2020].
- [56] ASM International Handbook Committee, *ASM Specialty handbook: Nickel, Cobalt, and Their alloys*. 2000.
- [57] Z. Tian *et al.*, "A review on laser powder bed fusion of inconel 625 nickel-based alloy," *Appl. Sci.*, vol. 10, no. 1, 2020, doi: 10.3390/app10010081.
- [58] ASTM International, "ASTM F3056 - 14e1 - Standard Specification for Additive Manufacturing Nickel Alloy (UNS N06625) with Powder Bed Fusion," *ASTM Standards*. United States, 2014, doi: 10.1520/F3056-14E01.
- [59] G. Marchese *et al.*, "Influence of heat treatments on microstructure evolution and mechanical properties of Inconel 625 processed by laser powder bed fusion," *Mater. Sci. Eng. A*, vol. 729, no. July 2017, pp. 64–75, 2018, doi: 10.1016/j.msea.2018.05.044.
- [60] H. Hack, R. Link, E. Knudsen, B. Baker, and S. Olig, "Mechanical properties of additive manufactured nickel alloy 625," *Addit. Manuf.*, vol. 14, pp. 105–115, 2017, doi: 10.1016/j.addma.2017.02.004.
- [61] J. A. Gonzalez, J. Mireles, S. W. Stafford, M. A. Perez, C. A. Terrazas, and R. B. Wicker, "Characterization of Inconel 625 fabricated using powder-bed-based additive manufacturing technologies," *J. Mater. Process. Technol.*, vol. 264, no. August 2017, pp. 200–210, 2019, doi: 10.1016/j.jmatprotec.2018.08.031.
- [62] SLM Solutions Group AG, "Material Data Sheet: Ni-Alloy IN625 / 2.4856 / B446," 2019. [Online]. Available: <https://www.slm-solutions.com/en/products/accessories-consumables/slmr-metal-powder/>. [Accessed: 25-Jun-2020].
- [63] E. Hosseini and V. A. Popovich, "A review of mechanical properties of additively manufactured Inconel 718," *Addit. Manuf.*, vol. 30, no. August, p. 100877, 2019, doi: 10.1016/j.addma.2019.100877.
- [64] M. E. Aydinöz *et al.*, "On the microstructural and mechanical properties of post-treated additively manufactured Inconel 718 superalloy under quasi-static and cyclic loading," *Mater. Sci. Eng. A*, vol. 669, pp. 246–258, 2016, doi: 10.1016/j.msea.2016.05.089.
- [65] ASTM International, "ASTM F3055 - 14a - Standard Specification for Additive Manufacturing Nickel Alloy (UNS N07718) with Powder Bed Fusion," *ASTM Standards*. United States, 2014, doi: 10.1520/F3055-14A.
- [66] W. M. Tucho, P. Cuvillier, A. Sjolyst-Kverneland, and V. Hansen, "Microstructure and hardness studies of Inconel 718 manufactured by selective laser melting before and after solution heat treatment," *Mater. Sci. Eng. A*, vol. 689, no. February, pp. 220–232, 2017, doi: 10.1016/j.msea.2017.02.062.
- [67] Z. Xu, J. W. Murray, C. J. Hyde, and A. T. Clare, "Effect of post processing on the creep performance of laser powder bed fused Inconel 718," *Addit. Manuf.*, vol. 24, no. October, pp. 486–497, 2018, doi: 10.1016/j.addma.2018.10.027.
- [68] T. G. Gallmeyer, S. Moorthy, B. B. Kappes, M. J. Mills, B. Amin-Ahmadi, and A. P. Stebner, "Knowledge of process-structure-property relationships to engineer better heat treatments for laser powder bed fusion additively manufactured Inconel 718," *Addit. Manuf.*, vol. 31, no. August 2019, p. 100977, 2020, doi: 10.1016/j.addma.2019.100977.
- [69] SLM Solutions Group AG, "Material Data Sheet: Ni-Alloy IN718 / 2.4668," 2019. [Online]. Available: <https://www.slm-solutions.com/en/products/accessories-consumables/slmr-metal-powder/>.

- consumables/slmr-metal-powder/. [Accessed: 30-Jun-2020].
- [70] EOS GmbH, "Material Data Sheet: EOS NickelAlloy IN718," 2020. [Online]. Available: <https://www.eos.info/en/additive-manufacturing/3d-printing-metal/dmls-metal-materials>. [Accessed: 01-Jul-2020].